



This is a repository copy of *On the formation of sand ramps: A case study from the Mojave Desert.*

White Rose Research Online URL for this paper:  
<http://eprints.whiterose.ac.uk/96000/>

Version: Accepted Version

---

**Article:**

Bateman, M.D., Bryant, R.G., Foster, I.D.L. et al. (2 more authors) (2012) On the formation of sand ramps: A case study from the Mojave Desert. *Geomorphology*, 161-16. pp. 93-109. ISSN 0169-555X

<https://doi.org/10.1016/j.geomorph.2012.04.004>

---

Article available under the terms of the CC-BY-NC-ND licence  
(<https://creativecommons.org/licenses/by-nc-nd/4.0/>)

**Reuse**

Unless indicated otherwise, fulltext items are protected by copyright with all rights reserved. The copyright exception in section 29 of the Copyright, Designs and Patents Act 1988 allows the making of a single copy solely for the purpose of non-commercial research or private study within the limits of fair dealing. The publisher or other rights-holder may allow further reproduction and re-use of this version - refer to the White Rose Research Online record for this item. Where records identify the publisher as the copyright holder, users can verify any specific terms of use on the publisher's website.

**Takedown**

If you consider content in White Rose Research Online to be in breach of UK law, please notify us by emailing [eprints@whiterose.ac.uk](mailto:eprints@whiterose.ac.uk) including the URL of the record and the reason for the withdrawal request.



[eprints@whiterose.ac.uk](mailto:eprints@whiterose.ac.uk)  
<https://eprints.whiterose.ac.uk/>

# On the formation of sand ramps: A case study from the Mojave Desert

Mark D. Bateman<sup>1</sup>, Robert G. Bryant<sup>1</sup>, Ian D.L. Foster<sup>2,3</sup>, Ian Livingstone<sup>2</sup>, Anthony Parsons<sup>1</sup>

<sup>1</sup> Geography Department, University of Sheffield, Winter St., Sheffield S10 2TN, UK.

<sup>2</sup>School of Science and Technology, The University of Northampton, Northampton NN2 6JD, UK.

<sup>3</sup> Geography Department, Rhodes University, Grahamstown 6140, Eastern Cape, South Africa

*\*Corresponding author*

This is an author produced version of a paper which was subsequently published in *Geomorphology*. This paper has been peer-reviewed but does not contain final published proof-corrections or journal pagination.

---

## Abstract

Sand ramps are dune-scale sedimentary accumulations found at mountain fronts and consist of a combination of aeolian sands and the deposits of other geomorphological processes associated with hillslope and fluvial activity. Their complexity and their construction by wind, water and mass movement means that sand ramps potentially hold a very rich store of palaeoenvironmental information. However, before this potential can be realised a full understanding of their formation is necessary. This paper aims to provide a better understanding of the principal factors influencing the development of sand ramps. It reviews the stratigraphic, chronometric and sedimentological evidence relating to the past development of sand ramps, focussing particularly on Soldier Mountain sand ramp in the Mojave Desert, as well as using observations of the modern movement of slope material to elucidate the formation of stone horizons within sand ramps.

Findings show that sand ramps cannot easily be interpreted in terms of a simple model of fluctuating palaeoenvironmental phases from aeolian dominated to soil/fluvial dominated episodes. They accumulate quickly (perhaps in  $5 \times 10^4$  ka), probably in a single phase before becoming relict. Based on the evidence from Soldier Mountain, they appear strongly controlled by a 'window of opportunity' when sediment supply is plentiful and cease to develop when this sediment supply diminishes and/or the accommodation space is filled up. Contemporary observations of stone movement both on rock and sandy sloping surfaces in the Mojave region indicate movement rates in the order of 0.6 and 11mm yr<sup>-1</sup>, which is insufficiently fast to explain how stone horizons could have been moved across and been incorporated into sand ramps on multiple occasions. Stone horizons found within the aeolian sediments lack evidence for soil development and are interpreted as very short-term events in which small streams moved and splayed discontinuous stone horizons across the sand ramp surface before aeolian deposition resumed. Surface stone horizons may form by creep from mountain slope sources across sand ramps but require enhanced speed compared to measured rates of runoff creep. We propose the mechanism of fluvio-aeolian creep. Our study suggests that current models of alternating Aeolian and colluvial deposition within sand ramps, their palaeoenvironmental significance and indeed how sand ramps are distinguished from other dune forms require amendment.

**Keywords:** Sand ramp, Talus, Aeolian, Dune, Luminescence, Mojave Desert

---

## 1. Introduction

Sand ramps are dune-scale sedimentary accumulations found at mountain fronts and consist of a combination of aeolian sands (from multiple or single sources) and the deposits of other geomorphological processes associated with hillslope and fluvial activity. The Aeolian material is trapped by the topography in the same manner as obstacle dunes fixed by topography (either 'climbing' or 'falling'). However, contrary to the suggestion of [Livingstone and Warren \(1996\)](#) that sand ramps may be seen as a sub-category of falling or climbing dune, they are actually far more complex. In addition to the input of Aeolian material, the mountain slopes above the ramp generate debris which is brought onto the ramp by either hydrological or gravitational processes. As a consequence, sand ramps are usually composed of a mix of Aeolian sand, talus deposits, debris flows, colluvium and fluvial deposits. Indeed, sand ramps might be viewed as lying on a continuum between endpoints created, respectively, solely by aeolian

processes or solely by hillslope processes. At the aeolian end of this continuum would be mountain-front climbing or falling dunes. At the alluvial end of the spectrum would be a variety of features including talus cones and alluvial fans. Between these end points, sand ramps display a variety of Aeolian and hillslope sediments, and the relative importance of these inputs may vary over time. This complexity and their construction by wind, water and mass movement means that sand ramps potentially hold a very rich store of palaeoenvironmental information. However, before this potential can be realised a fuller understanding of their formation is necessary.

Against this background of uncertainty, the present study aims to discuss the geomorphological issues associated with the formation of sand ramps in order better to understand the principal factors influencing the development of sand ramps. It

aims to review and investigate further: [1] stratigraphic, chronological and sedimentological evidence relating to the past development and accumulation rates of sand ramps; [2] how observations of the modern movement of slope material elucidate the formation of stone horizons within sand ramps. (In this paper we use the term 'stone horizon' as equivalent to the 'stone band' or 'talus band' of others.)

**2. Previous work**

Sand ramps have been recognised in remarkably few desert environments. However, given that their surface may be either sandy or stony it is quite possible that they have gone unrecognised in many environments, being taken as either topographically-anchored dunes (with a sandy surface) or as alluvial fans or talus cones (with a stony surface). It is often only where exposures have been created, either by natural processes of incision or by human activity, particularly quarrying, that the true nature of these features has been recognised. While sand ramps have been widely studied in the Mojave, USA they also have been described from the central Sahara (Busche, 1998 cited by Bertram, 2003), the southern Namib (Bertram, 2003), Jordan (Turner and Makhlof, 2002), Iran (Thomas *et al.*, 1997), Mallorca (Clemmensen *et al.*, 1997) and South Africa (Telfer *et al.*, 2012).

The main focus for work on sand ramps has been the Mojave Desert, California, USA. The term sand ramp appears to have first been used by Tchakerian in his 1989 thesis on aeolian features in the Mojave Desert and was used in his subsequent papers and those of others in the 1990s. Here, the 'basin-and-range' topography provides ample opportunity for sediment to accumulate on mountain fronts by combining active hillslopes with aeolian sand transport. The first published discussion of these features was in the work of

Tchakerian (1991) followed subsequently by a series of reports on the use of luminescence techniques to provide a chronology (Clarke, 1994; Rendell *et al.*, 1994; Clarke *et al.*, 1996a, 1996b; Rendell and Sheffer, 1996; Clarke and Rendell, 1998) as well as some broader discussions of the geomorphology of the sand ramps (Lancaster and Tchakerian, 1996, 2003; Tchakerian and Lancaster, 2002).

Given the difficulty of recognising these features in the field and the paucity of previous work, it is not surprising that there are very considerable uncertainties associated with the formation of sand ramps. Although previous studies have invoked a combination of Aeolian and hillslope sediments, there does not appear to have been any systematic attempt to explain the mechanism(s) and speed by which horizons of stones moved by water and/or gravity can be moved into aeolian deposits. This lacuna is not helped by the lack of data on accumulation rates for sand ramps as aeolian geomorphologists have concentrated on dune forms where measurable (in the short-term) sediment accumulation rates have been observed (Wiggs, pers. comm.). Thus to gain insight into net accumulation rates it is necessary to turn to 'palaeo' records and the limited number of sites that have multiple ages from single sedimentary profiles/units (Fig. 1). Using this previous work to understand the aeolian-colluvial/fluuvial interplay, however, is hampered by previously published chronologies having high age uncertainties (up to 30%, average around 12%), age reversals with depth and within units (e.g. Fig. 1a), as well as sampling strategies which do not always date upper and lower parts of stratigraphic units (e.g. Fig. 1e). To illustrate this point, Table 1 shows calculated minimum and maximum accumulation rates for the Dale Lake and Ardekan sand

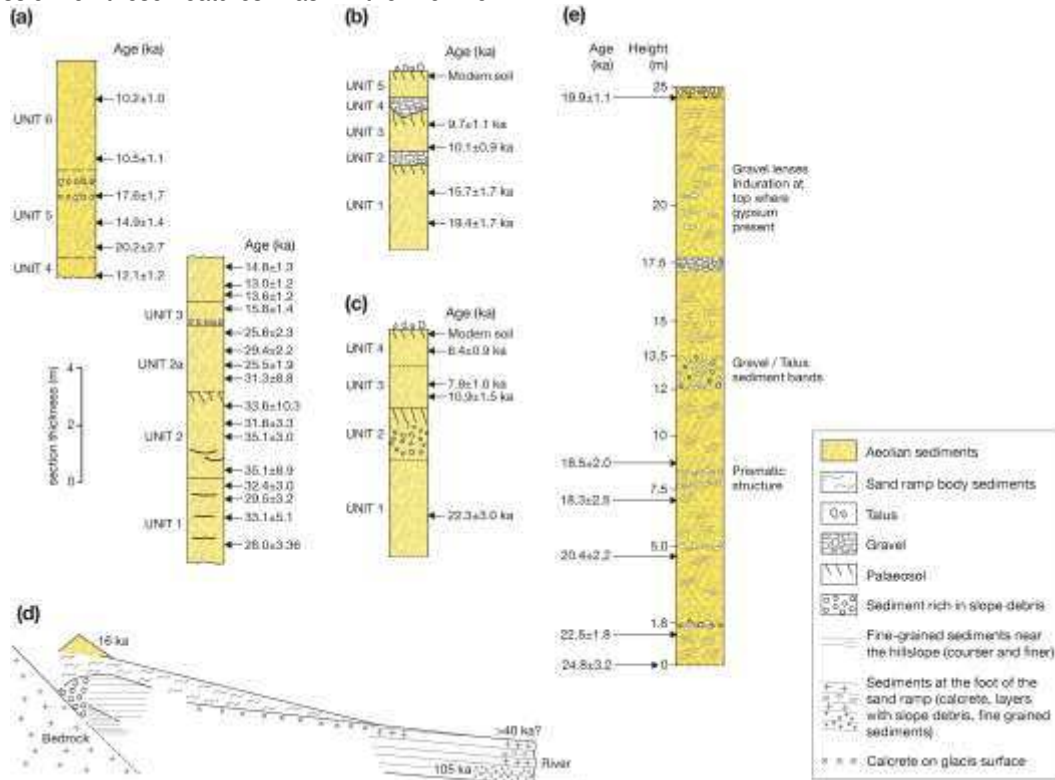


Fig. 1. Stratigraphical information and associated chronologies for selected sand ramps: (a) Dale Lake (after Rendell *et al.*, 1994, Fig. 2); (b) Iron Mountain (after Lancaster and Tchakerian, 2003); (c) Big Maria (after Lancaster and Tchakerian, 2003); (d) Aus sand ramp, Namibia (after Bertram, 2003, Fig. 149); (e) Ardekan sand ramp, Iran (after Thomas *et al.*, 1997, Fig. 5).

Table 1. Published accumulation rates for sand ramps

Unit	Sediment Thickness (m)	Max Age (ka)	Min Age (ka)	Min Accumulation Rate (m/ka)	Max accumulation Rate <sup>2</sup> (m/ka)
Dale Lake Sand Ramp, Mojave (Rendell <i>et al.</i> 1994)					
Unit 1	2.0	33.1 ± 5.1 <sup>1</sup>	28.0 ± 3.36 <sup>1</sup>	0.15	2.0
Unit 2	2.3	35.1 ± 8.9 <sup>1</sup>	31.6 ± 3.3 <sup>1</sup>	0.13	2.3
Unit 2a	1.6	31.8 ± 8.8 <sup>1</sup>	25.5 ± 1.9 <sup>1</sup>	0.09	1.6
Unit 3	-	-	-	-	-
Unit 4	1.0	14.8 ± 1.3 <sup>1</sup>	12.1 ± 1.2 <sup>1</sup>	0.20	5.0
Unit 5	1.85	20.2 ± 2.7 <sup>1</sup>	14.9 ± 1.4 <sup>1</sup>	0.20	1.5
Unit 6	2.05	10.5 ± 1.1 <sup>1</sup>	10.2 ± 1.0 <sup>1</sup>	0.85	2.1
Ardakan Sand Ramp, Iran (Thomas <i>et al.</i> 1997)					
Shfd95008-Shfd95009	1.25	24.8 ± 3.2 <sup>1</sup>	22.5 ± 1.8	0.17	1.25
Shfd95009-Shfd95011	3.50	22.5 ± 1.8	20.4 ± 2.2	0.57	3.50
Shfd95011-Shfd95012	2.50	20.4 ± 2.2	18.3 ± 2.5	0.37	2.50
Shfd95013-Shfd95014	15.75	19.1 ± 1.1 <sup>1</sup>	18.5 ± 2.0 <sup>1</sup>	4.63	15.75

<sup>1</sup> age reversals and ages within error of each other present in units so calculations based on minimum and maximum ages wherever they occurred in unit.

<sup>2</sup> Where ages are within errors maximum accumulation rate assumed to be that the total unit thickness was deposited within 1 ka.

ramps. Overall the chronologies show that individual sand ramp units can accumulate very rapidly (maybe as fast as ~2 m/ka) and that sand ramps form over the course of up to 20 ka (but often much less) before becoming relict features. However, while all the studied sand ramps have clear stratigraphical breaks between aeolian- and fluvial/colluvial derived sediments, suggesting phased accumulation, there is disagreement as to whether stone horizons represent significant temporal breaks in aeolian sedimentation or not and whether sufficient time has elapsed in order for proto-'soils' to start forming. While sufficient time would appear to be available for the Dale Lake, Iron Mountain and Big Maria sand ramps (Rendell *et al.*, 1994; Lancaster and Tchakerian, 2003; Fig. 1a–c), this does not appear to be the case for the Ardekan sand ramp (Fig. 1e).

Although the presence of discontinuous horizons of rock fragments at most a few fragments thick has been used as evidence of the interplay of fluvial, aeolian and hillslope processes in the formation of sand ramps, interpreting this interplay is problematic in two respects. First, there is the question of what processes are responsible for the presence of the coarse fragments, and secondly the issue is what they might indicate about the temporal relationships among the processes. There is some difference of opinion in the literature as to what these deposits represent. Whereas Lancaster and Tchakerian (1996) call them 'talus deposits' (sometimes associated with palaeosols) and use the same term to refer to the layer of coarse fragments that typically mantle sand ramps in the Mojave Desert, similar deposits on sand ramps in Namibia are referred to as 'desert pavement' (on the surface) and 'slopewash deposits' (within the body of the sand ramp) by Bertram (2003). Turner and Makhlof (2002) attribute 'stringers of boulders' on sand ramps in Jordan to the process of rockfall. The difference in attribution of these horizons of coarse particles is crucial for interpretation of the chronology of sand ramps. Rockfalls, like debris-flow deposits and (in the context of dryland environments) probably also fluvial deposits, may be characterised as event-based deposits. They are created in response to an individual storm event (in the case of debris flows and stream-channel deposits) or sudden failure of part of the headwall against which the sand ramp is accumulating (in the case of rockfall deposits). Thus, they provide no information about the chronology of sand-ramp formation, other than to indicate occasional high-magnitude events delivering coarse particles into an otherwise aeolian system. There is (also) some difficulty in interpreting these coarse particles as talus as they do not evidently accumulate close to their source and may be size sorted in places. Those in Jordan that have been interpreted as rockfall deposits are reported to fine in the downslope direction, which is contrary to the norm for rockfall deposits where the greater

momentum of the larger particles and their lower susceptibility to trapping typically carries them further (Selby, 1993: 353). More likely, the particles owe their origin to rockfall from the backing rock slope, but they owe their current location to subsequent transportation across the ramp surface, as suggested by Bertram (2003).

### 3. Study area

The field evidence in this investigation concentrates on a single sand ramp in the Mojave Desert at Soldier Mountain in the Cady Range, California, USA (grid ref: 34° 56' 21" N, 116° 34', 50" W, quarry elevation c. 550 masl) where quarrying has exposed the internal in situ sand ramp stratigraphy. This extensive access to the stratigraphy of a sand ramp is to the authors' knowledge without equal therefore providing a unique opportunity to understand better the processes associated with sand ramp formation. The site has been studied previously (e.g. Rendell and Sheffer, 1996; Lancaster and Tchakerian, 1996; Clarke and Rendell, 1998) and shown to be of considerable regional significance (e.g. Lancaster and Tchakerian, 2003), but these studies have not explicitly linked the sand ramp stratigraphy to the luminescence chronology. In addition, inferred aspects of the stratigraphy (e.g. the presence of palaeosols and horizons of talus bounding aeolian units; Lancaster and Tchakerian, 1996), and the general relationship of the sand ramp to the basin history in which it resides are somewhat ambiguous. Using this site as a type-example, therefore, the present study presents a new chronostratigraphy for the sand ramp to look at its accumulation history. Sediment particle size and magnetic characterisation are used to look for evidence of past soil development within the sand ramp, while luminescence dating is employed to bracket the stone horizons (the 'talus layers' of Lancaster and Tchakerian, 1996) to establish how quickly they formed. In addition, new data from a stone movement experiment allied to an understanding of regional slope processes are examined in order to improve understanding of any possible relationships between periods of stone horizon formation and periods of aeolian sediment deposition.

#### 3.1. Setting

Soldier Mountain forms part of a pre-Tertiary igneous and basement complex that is interrupted locally by a number of fault systems (e.g. Cady Fault and Manix/Afton Canyon Fault; Dokka and Travis, 1990). Hills of the Cady Range directly to the south and east of Soldier Mountain are mainly of similar lithology, interspersed with Tertiary volcanic and sedimentary sequences (Glazner *et al.*, 2002). The sand ramp is located on the western side of Soldier Mountain approximately 0.5 km

south of the current Mojave River channel which is assumed to be the single main source of aeolian derived material to the sand ramp. Dominant present-day sand-transporting winds in this region are consistently from a westerly direction (Zimbelman *et al.*, 1995).

In the context of the regional palaeoenvironment, the sand ramp sits on the eastern edge of the Lake Manix Basin upon which a range of studies have been undertaken (e.g. Meek, 1989; 1999; Jefferson, 2003; Reheis and Redwine, 2008; Fig. 2). This basin was the effective sump for the Mojave River system until the Late Pleistocene (Reheis and Redwine, 2008). High-stands for Lake Manix have been recorded up until 27–25 ka after which the Mojave system drained eastwards to the Lake Mojave Basin (Reheis *et al.*, 2007). The draining of Lake Manix led to the eventual cutting of Afton Canyon, the drying of Lake Manix, and the periodic filling of Lake Mojave, which itself eventually completely dried by 8.5 ka (Reheis and Redwine, 2008 and references therein). Past regional chronological assessments of aeolian systems in these basins (e.g. Lancaster and Tchakerian, 1996; Rendell and Sheffer, 1996; Clarke and Rendell, 1998; Kocurek and Lancaster, 1999) have linked aeolian sand transport and deposition in this region (including the emplacement of sand ramps) to the draining of Lakes Manix and Mojave, and the subsequent increased availability of sediment from the lake shorelines, exposed deltas and the ephemeral Mojave River (Enzel *et al.*, 2003; Wells *et al.*, 2003; Miller *et al.*, 2010).

Within the current Manix Basin there are two ephemeral lakes. Coyote Lake sits in a sub-basin approximately 20 km NW of Soldier Mountain, and Troy Lake sits approximately 10 km to the south (see Fig. 2). During the period directly after the draining of Lake Manix (24 ka to 14 ka; Reheis and Redwine, 2008), there is some evidence of periodic diversion of flow from the Mojave River both into Troy and Coyote Lake (e.g. Meek, 1989; 2004), with the latter matching periods in which Lake Mojave levels were known to fluctuate (e.g. Wells *et al.*, 2003; Miller *et al.*, 2010). It is also clear that the Mojave River changed course in this period (see Fig. 2 inset), and some evidence exists for the beginnings of stable channel emplacement at the current channel location to have occurred sometime between 15 and 12 ka (e.g. Reynolds and Reynolds, 1994; Reheis and Redwine, 2008; Miller and Dudash, 2009).

The sand ramp itself, in common with other similar ramps and topographically anchored aeolian deposits in the region, is mantled by a veneer of angular clasts which we assume to have been derived from the adjacent mountain front. The contact between the ramp's top surface and the mountain front displays sediments lapping directly onto the rock slope at angles between 5° and 11°. The sand ramp is cut by river channels emanating from the adjacent mountain front

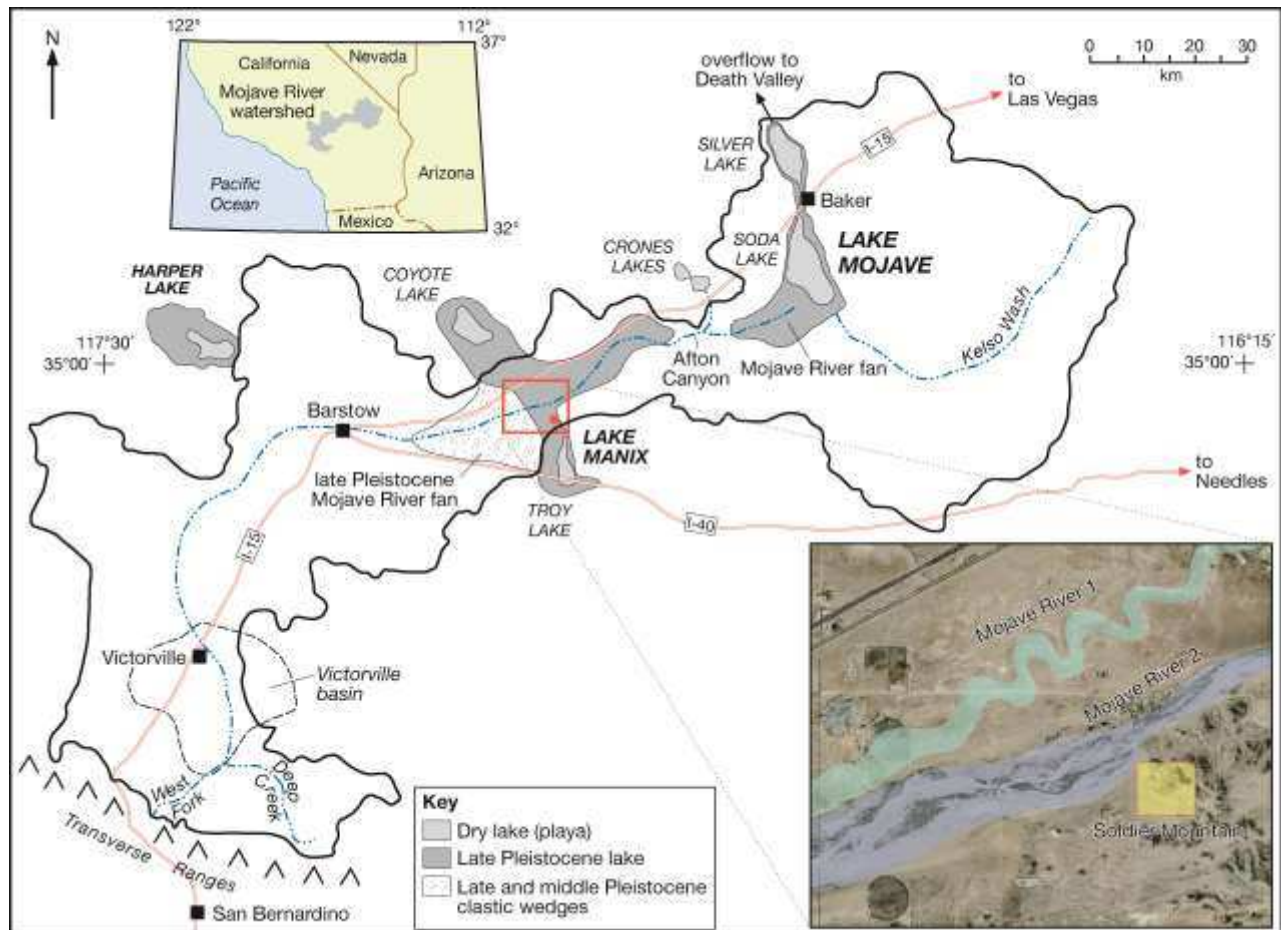


Fig. 2. The region of study within the Mojave, southern California. Mojave River surface drainage basin in southern California as proposed by Enzel *et al.* (2003). The location of Soldier Mountain at the eastern edge of the Manix Basin is noted as a red dot. The inset (red box) shows the location of Soldier Mountain within the Lake Manix Basin, and also illustrates the proximity of the sand ramp to past (Mojave River I; Reheis *et al.*, 2007) and present Mojave River (II) courses. The box shows the approximate area covered by Fig. 3. (Inset image courtesy of Google Earth).

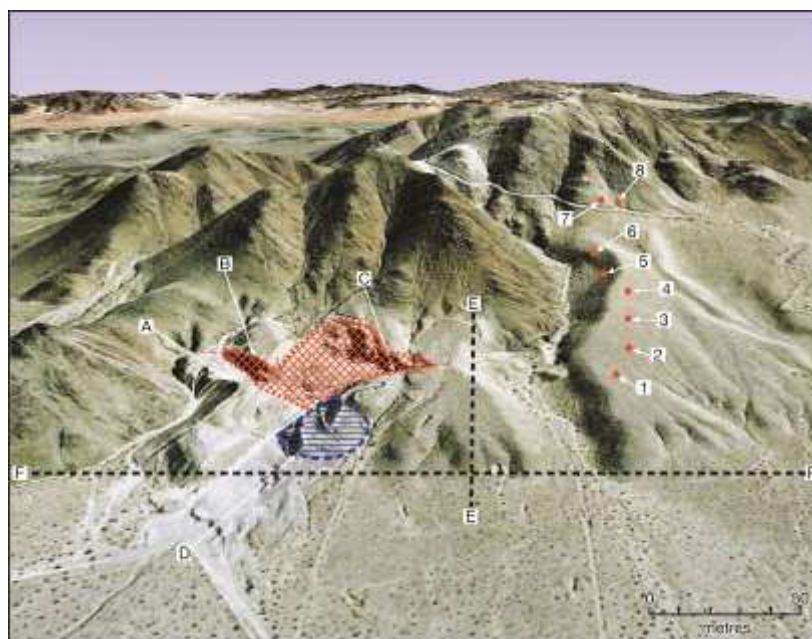


Fig. 3. A. 3D rendering of the location of stratigraphic/topographic sections and experimental sites at the Soldier Mountain sand ramp (general aspect towards the East). Quarry sections A, B and C (cross-hatched) are flagged. Area D (horizontal hatching) represents the approximate extent of unit Ia. Line E represents the location of a surface DGPS profile over the top of the sand ramp. Line F–F' represents the approximate location and orientation of the terrace at the base of the sand ramp. Points 1 to 8 represent the locations of experimental stonemovement measurement stations on the surface of the neighbouring sand ramp. Image courtesy of Google Earth.

which flow the short distance NW towards the Mojave River (see Figs. 2, 3). The ramp is also truncated at its western end by a terrace (Line F in Fig. 3; possibly the 543 m Lake Manix shoreline of Meek, 1989). The Soldier Mountain sand ramp has been worked as a quarry thereby revealing internal stratigraphy. On the opposite (eastern) side of Soldier Mountain to the sand ramp there is an active falling dune consisting of well-sorted coarse sands which represents contemporary transport of material from the nearby Mojave River.

#### 4. Stratigraphy

To elucidate the stratigraphy, a number of sections were logged in the Soldier Mountain quarry (see cross-hatched area in Fig. 3). The locations of these sections along with other key features of the site are recorded in Fig. 3. Sections A and B were obtained from vertical faces in the northern part of the quarry. Section C has been derived from vertical faces in the southern part of the quarry. Summary stratigraphic logs are presented in Fig. 4. The elevations of the top and bottom of each section, as well as a number of intermediate ledges, were derived using digital GPS, and all measurements were tied to USGS datum. A number of cross-sections of the top surface of the sand ramp were also surveyed, and one of these (E to E' in Fig. 3) is used here as an example. Details of the main stratigraphic units described in these sections are outlined below, and compared directly to previous work. Photographs outlining some of the sedimentological characteristics of each unit are provided in Fig. 5.

##### 4.1. Basal units Ia and Ib

In the base of the quarry two principal units were observed. The first (Ia) is a red brecciated igneous deposit that was exposed at the entrance to the quarry (Fig. 3 point D). Unit Ia is assumed to be at least of Tertiary age. The second unit (Ib) formed the quarry floor, with limited exposures in the northern

and central parts of the quarry (sections A and B; Fig. 4). This unit comprises a weakly bedded grey/blue fine-grained deposit, the top of which rarely exceeds 546 masl. Unit Ib is interpreted as being former Lake Manix sediment, which conforms to Reheis and Redwine (2008) who noted local Lake Manix high-stands (indicated by beach ridges) at 543 and 557 masl (using the same elevation datum as this paper).

##### 4.2. Unit II

Lying directly above these basal units is a heterogeneous but pervasive 2–3 m-thick unit (II) which includes locally-derived coarse angular boulders and pebbles in a sandy matrix, varying from clast-supported to matrix-supported in section. This unit is interpreted as a debris flow unit as within it could be seen occasional, exposed cross-sections through channelised/confined debris flow events (see Fig. 5a) which varied in size from 1 to 5 m in width. These cross-sections display typical levée and channel deposits indicative of multiple phases of transport. The unit was exposed clearly in both the northern and southern parts of the quarry (sections A, B and C), and is equivalent to unit 1 of Lancaster and Tchakerian (1996) (Fig. 4). The contact between this unit and units Ia/b (Fig. 5a) is normally quite sharp, and the contact surface often undulose in cross-section. In terms of process, this unit suggests the existence of high runoff on steep slopes with substantial debris available for mobilisation.

##### 4.3. Unit III

This unit has a relatively sharp contact with unit II, and is approximately 6–8 m in thickness. The key components of the unit are: (a) thinly bedded and generally well sorted medium/fine aeolian sands interspersed with (b) layers of coarse, angular, locally-derived non-aeolian clasts (termed 'talus' by Lancaster and Tchakerian, 1996, and called stone horizons here) that are variable in their distinctness and length, and (c) nodular calcrete with root traces (interpreted as

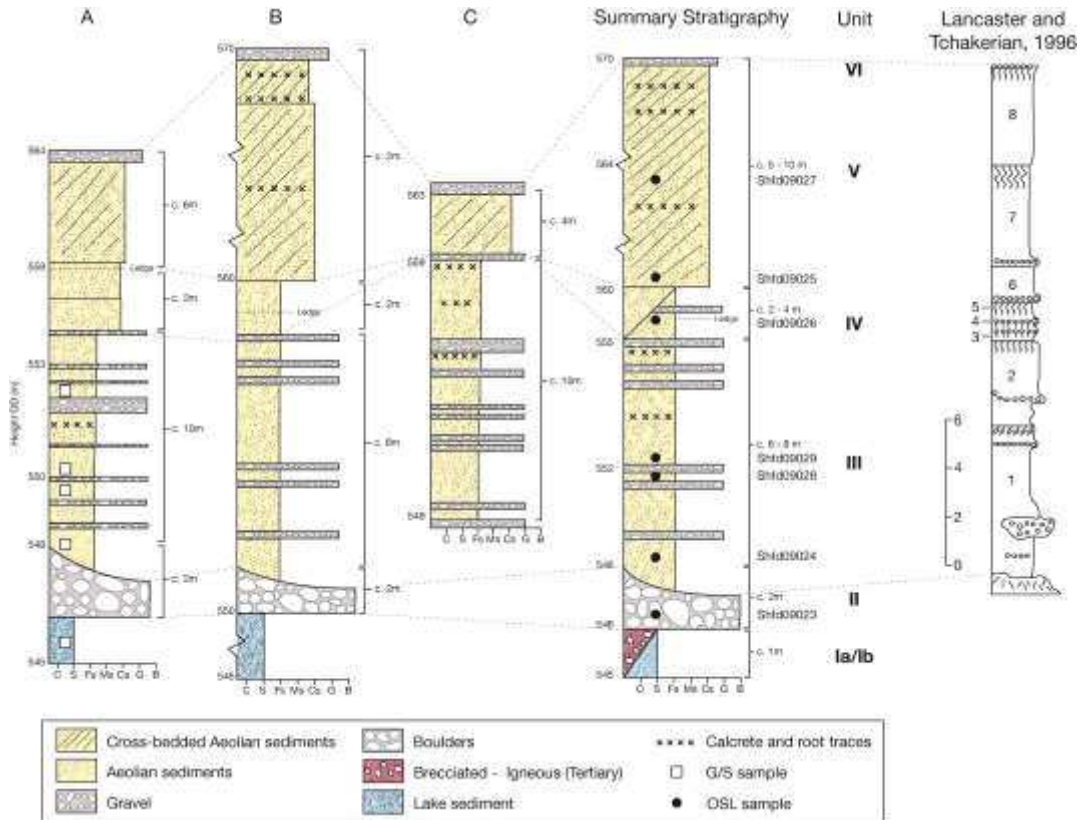


Fig. 4. Summary stratigraphy for the Soldier Mountain sand ramp, outlining the major units exposed. Sections A and B are a summary of stratigraphic logs taken from the vertical faces exposed the northern part of the quarry. In section A, the square boxes represent sample locations for grain size analysis. Section C is a summary of logs taken from the southern part of the quarry. A summary stratigraphy for the central part of the Soldier Mountain deposit is also provided, as well as (for reference) a comparison section from Lancaster and Tchakerian (1996). Figures next to the sections are the DGPS altitudes in masl relative to local Ordnance Datum for exposed ledges and stratigraphic boundaries. Locations of grain size samples (G/S) and luminescence samples (OSL) are also noted.

rhizocretions) which are inferred to have formed at the near-surface (Nash, 2011). Some of these angular stone horizons provide a semi-continuous (over 8–12 m in section on some occasions) stratigraphic markers with a thickness of 1–2 clasts within the sequence of Aeolian sands (e.g. section A; Fig. 5c). If these stone horizons were of true talus origin then it would be assumed that they formed through rockfall or avalanching of material to the surface of the sand ramp from the adjacent mountain front. In some instances these stone horizons with angular clasts are associated with poorly developed nodular calcrete layers which often display evidence of root traces (see Fig. 5b). However, more often than not the angular stone horizons were seen to be discontinuous in section. In addition, calcrete layers were also commonly observed in the absence of angular clastic material; especially in the upper part of the unit on the southern side of the quarry. Thus, based on initial stratigraphic observations alone, the direct association between the stone horizons and the aeolian sediments and calcrete deposits immediately in their vicinity was not easy to infer; nor was the mechanism whereby the clasts have been emplaced. On occasion, small (b1 m wide) constrained alluvial/fluvial channel deposits of sand and pebbles were observed in this sequence, suggesting that some surface flow of larger clasts was possible. However, these channel deposits were often found in apparent isolation within the aeolian sequences, seemed to cross cut them, and were rarely seen to be directly stratigraphically linked to the stone horizon units which often bracketed them. In summary, our assessment of the non-aeolian

sediments within unit III suggested that significant further work was required in order to understand the processes leading to their emplacement. This unit is broadly equivalent to units 2–5 of Lancaster and Tchakerian (1996) (see Fig. 4).

#### 4.4. Unit IV

This is a 2–3 m-thick unit of thinly bedded and generally well sorted medium sands largely devoid of angular stone clasts or horizons (Fig. 5c). The lower part of this unit is light pink, while the upper part bleached/white. This unit was most clearly observed in the northern part of the quarry (sections A and B; Fig. 4). In the southern part of the quarry (section C) the unit is not apparent, which could indicate pinching out to the south, perhaps indicative of a more northerly influence of the source. The upper part of this unit contains abraded ostracods (identified as *Limnocythere ceriotuberosa*, a species which dominates the Lake Manix core; Reheis and Redwine pers. comm.). This unit is interpreted as an aeolian unit which includes material re-worked from Lake Manix deposits. Generally, it is equivalent to unit 6 of Lancaster and Tchakerian (1996) (see Fig. 4).

#### 4.5. Unit V

This unit of well sorted, medium sand is between 5 and 10 m thick, and sits above a sharp contact with units IV (northern part of the quarry) and III (southern part of the quarry; see Figs. 3, 4). It is pink/red, lacks angular clasts and, in the southern part of the quarry

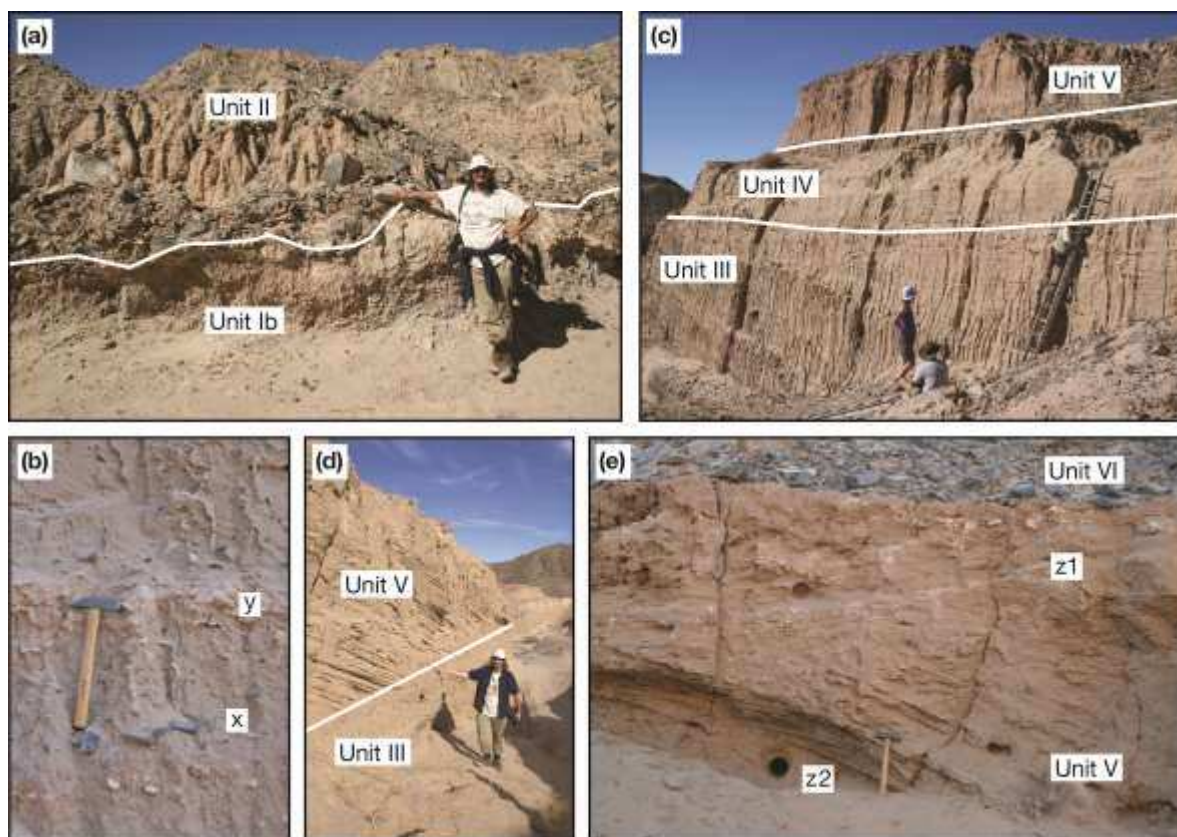


Fig. 5. Sedimentological characteristics of units within the Soldier Mountain Sand Ramp showing: (a) the contact between units Ib and II; (b) the presence of angular clasts (x) and calcrete nodules/rhizocretions (y) within unit III; (c) the location of unit IV in section A and its stratigraphic relationship with unit III and unit V; (d) the sharp contact between unit III and unit V in the southern part of the quarry highlighting the well exposed tabular foresets in the upper unit; (e) a close up of a portion of unit V showing the presence of calcrete associated with some of the bedding planes (z1), the overlying coarse material on the surface of the sand ramp (unit VI) and the location of luminescence sample points (z2).

in particular, is cross-bedded (see Fig. 5d) with nodular calcrete layers on the surfaces of some of the foresets (see Fig. 5e). The foresets indicate an approximate south or south easterly sand transport direction with free bedform migration over the surface of the sand ramp. The presence of free dunes on the surface of sand ramps has been observed as a component of the top surface stratigraphy of sand ramps by Bertram (2003), and can also be observed on the surface of the sand ramp in the East Cronese Basin, Mojave, USA (35° 08' 03" N, 116° 17', 30" W; see Clarke *et al.*, 1996a, 1996b). In the southern part of the quarry, the cross-bedded unit is mantled directly at the surface by coarse locally-derived angular clasts. In the northern part of the quarry it is overlain by a more massive unit of similar hue that was less obviously cross-bedded and then a top surface of locally-derived angular clasts. These units are equivalent to units 7 and 8 of Lancaster and Tchakerian (1996) (see Fig. 4).

#### 4.6. Unit VI

Directly on top of unit V there is a continuous unit of coarse, angular and often tightly packed clasts (thickness 1–2 clasts) which mantle the entire sand ramp. Generally, the clast size decreases down-slope from the mountain front (with mean clast size in the range 40–60 mm), and in some places in this unit we see some evidence of soil and desert pavement development directly below this. This unit is cut by the incised channels which dissect the sand ramp. Similar units have been described on the surface of all sand ramps in the Mojave (Lancaster and Tchakerian, 2003; see Fig. 1a), and Bertram(2003) describes consistent debris cover and rock

fragments associated with desert pavements on the top of Namibian sand ramps. Similarly, Thomas *et al.* (1997) also describe 'talus gravels' of a similar nature on the top surface of sand ramps in Iran (see Fig. 1e).

#### 4.7. The significance of stratigraphical interpretations of the development of the Soldier Mountain Sand Ramp

From these data and logs it can be seen that stratigraphy of the Soldier Mountain sand ramp does indeed record an interplay of aeolian, fluvial and debris-flow processes, with the distinct likelihood of multiple sediment sources. At the base of the quarry there is clear evidence for a period of debris flows from the adjacent mountain front directly overlying Lake Manix sediments (or an older brecciated igneous feature). Above this a significant accumulation of aeolian sand is observed with evidence of aeolian re-working of Lake Manix sediments. In this unit evidence for occasional periods of constrained fluvial deposition is also seen, which suggest the existence of some rainfall events which are large enough to transfer/deposit material from the mountain front onto the surface of the sand ramp. At the top of the quarry there is clear evidence for the existence of free dunes migrating over the surface of the sand ramp, perhaps with a different source location. Throughout the upper part of the sand ramp sequence is evidence of nodular calcrete and rhizocretion formation at or near the sediment surface, suggesting some element of seasonal/occasional wetting and temporary surface stability on the sand ramp surface. However, the most intriguing components of the stratigraphy at this site, which are less straightforward to

Table 2. Luminescence ages from Soldier Mountain sand ramp (Rendell and Sheffer, 1996). Note ages are ranked by depth and those emphasised in bold are those selected for the palaeoenvironmental reconstruction of Clarke and Rendell (1998).

Sample Code	Depth (m)	Quartz TL (ka)	Feldspar TL (ka)	Feldspar IRSL (ka)
SM04	1.0	11.45 ± 1.55	7.72 ± 1.38	6.74 ± 0.91
SM05	2.4	19.80 ± 2.67	15.38 ± 2.02	<b>11.14 ± 1.50</b>
SM01	7.0	10.34 ± 1.39		<b>15.88 ± 2.14</b>
SM02	7.5	19.55 ± 2.64		<b>20.24 ± 2.73</b>
SM03	7.7	7.46 ± 1.010	7.52 ± 1.02	<b>11.39 ± 1.53</b>
SM06	9.1			<b>20.06 ± 2.70</b>
SM07	10.2	15.60 ± 2.10	9.89 ± 1.33	<b>12.45 ± 1.68</b>
SM08	10.7			14.01 ± 1.89
SM09	12.2	20.82 ± 2.81		<b>19.43 ± 2.62</b>
SM10	14.3		23.20 ± 3.13	<b>13.00 ± 1.75</b>
SM11	15.1			<b>14.31 ± 1.93</b>
G28	16.5	21.50 ± 2.92	23.08 ± 3.12	<b>22.62 ± 3.05</b>
SM12				
SM13	18.5	18.60 ± 2.51	25.98 ± 3.50	
SM14	19.0	20.29 ± 2.74		<b>21.05 ± 2.84</b>

interpret, are: (i) the presence of a large number of discontinuous stone horizons made up of locally-sourced angular clasts which are mostly found within the intermediate aeolian unit (III), and (ii) the absence of any real evidence for palaeosols that can be directly associated with them (in units III, IV or V).

### 5. Sand ramp chronology

Previous age determinations for the Soldier Mountain site (Rendell and Sheffer, 1996) were undertaken to provide a chronology for the sand ramp rather than to understand the temporal component of the stone horizons (Table 2). For the present study new samples were collected for OSL targeting just above and below stone horizons, to see, in addition to checking the site chronology, if it was possible to establish whether the stone horizons represented a significant temporal hiatus in sedimentation or not.

#### 5.1. OSL methodology

Quartz was extracted and cleaned from the new Soldier Mountain samples under low-intensity red lighting at the Sheffield Centre for International Drylands Research Luminescence Laboratory. To achieve this extraction, organics and carbonates were removed with HCl and H<sub>2</sub>O<sub>2</sub>, and quartz was separated from heavy minerals with a density separation using sodium polytungstate (S.G. 2.7 g cm<sup>-3</sup>). A 45-minute 40% HF etch and sieving was used to remove heavily etched lighter minerals. No significant contamination was observed when prepared samples were tested using infrared stimulated luminescence. OSL measurements were carried out with a TL-DA-15 Risø automated luminescence reader with stimulation via blue diodes and signal detected through a 7.5 mm Hoya U340 filter. De values were derived using the single aliquot regeneration (SAR) protocol (Murray and Wintle, 2003) with four regeneration points and a recycling dose and an experimentally determined preheat

temperatures of 180 °C for 10 s. Multiple replicates of each sample were measured (minimum of 24 aliquots) to give an indication of De reproducibility. All samples exhibited OSL decay curves dominated by the fast component and therefore rapidly bleachable, low thermal transfer and good recycling. The replicate De distributions of all samples are normal with an additional few(1–3) aliquots with larger De values. The latter were regarded as outliers and excluded from further analysis. Based on these distributions and low over-dispersion (OD) values (average OD=15%) the samples are considered to have been reset prior to burial. The central age model (Galbraith *et al.*, 1999) was used to generate mean De values for the final age calculations.

Dose rates were determined from in situ field measurements made with an EG&G Micromad field gamma-spectrometer and attenuated for sediment size and palaeo-moisture contents (based on present day values with a 2% absolute error to incorporate any past changes; Table 3). Gamma-spectrometer results were compared to those obtained with ICP-MS. Comparison between these two techniques returned ratios within errors of unity for K (0.95±0.07) and Th (1.03±0.3) validating the assumption that the dose rate is in secular equilibrium for these two elements. While U was a little low (0.9±0.3) it is thought this small discrepancy may reflect the fact that ICP measured the sediment sampled while the gamma-spectrometer measured sediment in a wide sphere around the sample, which is more likely to incorporate any heterogeneity within the sediment. Cosmic dose rates were determined following published algorithms (Prescott and Hutton, 1994).

#### 5.2. Chronological interpretations of the development of the Soldier Mountain sand ramp

As shown in Table 3, ages are presented with one sigma uncertainties in ka from the year of measurement (2009). Results, with one exception, show an increase in age with depth. The age from the debris-flow derived sediment underlying the sand ramp (unit II; Shfd09023; 15.0±1.0 ka) indicates that this deposit is significantly older than the overlying sand ramp sediments (Fig. 4) forming at a time after the demise of Lake Manix but while significant overland flow was occurring. The ages from unit III (the main body of the sand ramp) have a maximum range of 11.6±0.8 ka to 8.3±0.6 ka (although the stratigraphically highest sample from unit III returned an age of 10.3±0.7 ka). The cross-bedded sand unit (unit IV) has an age of 9.5±0.6 ka. These new OSL results are consistently younger than those reported by Rendell and Sheffer (1996; Table 2). Whereas the chronology of Rendell and Sheffer (1996; Table 2) indicated that Soldier Mountain developed over a 10 ka period between ~10 and 22 ka. The new OSL chronology implies a much younger and more rapidly accreting chronology

Table 3. OSL related data and ages.

Unit	Lab. Code	Depth (m)	Water content (%)	K (%)	U (%)	Th (ppm)	Total dose rate <sup>a</sup> (Gy ka <sup>-1</sup> )	N <sup>b</sup>	D <sub>0</sub> (Gy)	OD <sup>c</sup> (%)	Age (ka)
IV	Shfd09027	5.0	0.5±2	2.61	1.52	7.93	3.26±0.18	19(20)	31.24±0.78	11	<b>9.5±0.6</b>
III	Shfd09025	6.5	0.6±2	2.64	1.66	7.79	3.26±0.18	17(20)	33.6±1.04	13	<b>10.3±0.7</b>
III	Shfd09026	7.9	0.3±2	2.89	1.62	7.04	3.43±0.20	15(18)	28.51±1.06	14	<b>8.3±0.6</b>
III	Shfd09029	15.9	0.2±2	3.03	1.58	7.90	3.61±0.21	20(21)	41.1±1.90	21	<b>11.4±0.8</b>
III	Shfd09028	16.3	0.2±2	3.01	1.38	7.23	3.55±0.21	18(21)	41.21±1.51	15	<b>11.6±0.8</b>
III	Shfd09024	19.6	0.6±2	2.77	1.70	8.59	3.39±0.19	17(20)	48.16±1.4	15	<b>11.3±0.8</b>
II	Shfd09023	18.5	0.6±2	2.74	2.67	6.5	3.26±0.18	20(20)	49.31±1.72	15	<b>15.0 ±1.0</b>

<sup>a</sup> Dose rate based on analysis of sediment by *in situ* gamma-spectroscopy and verified with ICP-MS.

<sup>b</sup> number of replicates upon which D<sub>0</sub> is based. Number in parenthesis indicates number of aliquots which met the quality control criteria (high signal to noise ratio, low thermal transfer, good and consistent growth of OSL with increasing laboratory doses, good recycling low palaeodose error and excludes outlier aliquots which fell beyond 2 standard deviations of the mean De).

<sup>c</sup> Over dispersion of De data excluding outlier aliquots which were beyond 2 standard deviations of mean.

for the sand ramp forming in the period between ~11.6–8.3 ka and probably 11.6–10.3 ka. It is hard to correlate exactly the new results with those of Rendell and Sheffer (1996) due to the lack of stratigraphical information provided by the latter. However, it is noted that the chronology of Rendell and Sheffer (1996) has high age uncertainties and age reversals, probably in part reflecting the older luminescence methods employed (multiple aliquot thermoluminescence (TL) and to a lesser extent, infra-red stimulated luminescence (IRSL)) which have greater potential to incorporate within them any antecedent signal unrelated to burial age (Lian and Roberts, 2006). This is of concern given some sand ramp sediment is of colluvial/fluvial origin and full exposure to sunlight prior to burial cannot be assumed. IRSL is now known to suffer from sensitivity changes and anomalous fading problems lead to age underestimation problems (Lian and Roberts, 2006; Lamothe and Auclair, 1999). The new ages, through use of the more light sensitive quartz and the OSL and through basing the ages on multiple single aliquot replicates (minimum 24) from which outliers were excluded, we believe to have better mitigated any effects of antecedent signal unrelated to burial age. The new OSL data (when taking into account their associated error limits) also appear more stratigraphically consistent (with only one age reversal), have smaller uncertainties and fit well with independent palaeoenvironmental data from the region (see discussion below; Fig. 11), and thus have been adopted for following discussion purposes.

Overall the new chronology indicates rapid accumulation of the sand ramp over a maximum period (taking into consideration age uncertainties) of less than 5 ka and more probably less than 3.4 ka (based on age of uppermost sample). Sediments from 19.6 m to 15.9 m (Shfd09024, Shfd09028, Shfd09029) are within errors of each other and appear to have been deposited around 11.4±0.8 ka with a sedimentation rate between 1.74 and 3.3 m/ka. Sediments above this group are younger ranging in age from 8.3±0.6 to 10.3±0.7 ka. Unfortunately, the upper paired samples above and below stone horizons, show an age reversal. However, the lower pair (Shfd09028 and Shfd09029) are almost identical in age and are within one sigma errors of each other. If age uncertainties are taken into consideration, this result indicates that the stone horizons represent a maximum of 1.8

ka and probably a much shorter time period based on the number of other stone horizons, the lack of identifiable soils (see section 6.1 below) and the interpreted maximum time it took to accumulate the whole sand ramp.

## 6. Sedimentological characteristics

Lancaster and Tchakerian (1996) identified six “palaeosols” in the Soldier Mountain sand ramp beneath the level of the cross-bedded sand of unit V, often beneath ‘talus’ (stone) horizons. They argued that the presence of palaeosols indicated periods of geomorphic stability of the sand ramp during the Late-glacial period. However, no direct supporting evidence was presented in order to confirm the interpretation and, as already seen, the chronology of Rendell and Sheffer (1996) fails to convincingly support (due to age reversals and large error certainties) Lancaster and Tchakerian’s contention. As also discussed above, the uncertainties associated with the new OSL data bracketing stone horizons still leave potentially hundreds and perhaps more than a thousand years for soil development associated with the stone horizons if these do indeed represent palaeo-surfaces. To investigate whether palaeosurfaces are associated with the stone horizons, particle size and magnetic susceptibility were employed to characterise the sediments and establish the location and nature of any palaeosols.

### 6.1. Mineral-magnetic and particle size methods

Many studies of Late Quaternary palaeosols have used mineral magnetic measurements in order to confirm their presence in loess deposits (e.g. Evans *et al.*, 1997; Dearing *et al.*, 2001; Evans and Heller, 2001; Maher *et al.*, 2003; Feng *et al.*, 2004; Avramov *et al.*, 2006; Jordanova *et al.*, 2007), and several studies have reported enhancement of magnetic susceptibility and frequency-dependent susceptibility in soils that are attributable to climate and pedogenesis (e.g. Maher, 1986; Maher *et al.*, 1994; Dearing *et al.*, 1996; Singer *et al.*, 1996; Walden *et al.*, 1998; Oldfield, 2007). To our knowledge no attempt has been made to make similar measurements on palaeosols in sand ramps and only a small number of studies (e.g. Sandgren and Thompson, 1990; Newsome and Walden, 2000) have attempted to

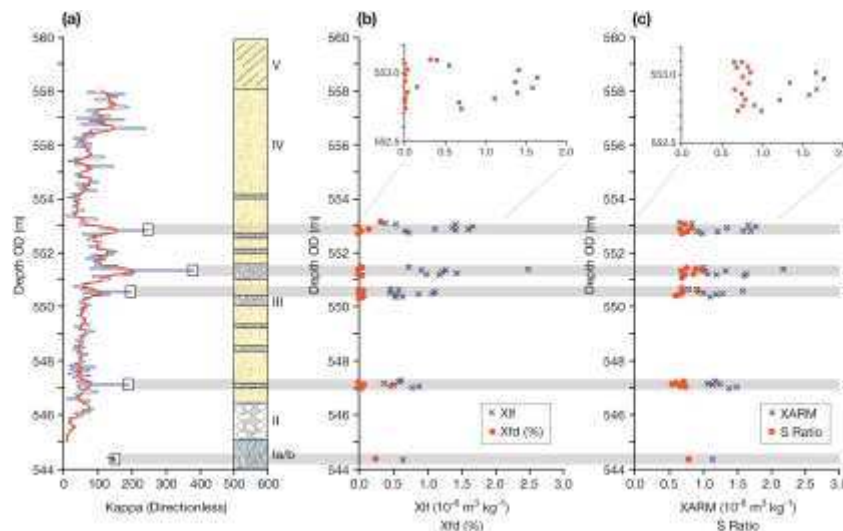


Fig. 6. Magnetic characterisation data. (a) Magnetic susceptibility  $\kappa$  on the section A profile of the Soldier Mountain sand ramp (raw data and a 3-point moving average alongside basic stratigraphic units; see Fig. 4 for key and further detail). Square boxes represent sample locations for environmental magnetism. (b) and (c) represent selected mineral magnetic characteristics of samples taken from 4 ‘palaeosols’ within unit III, and one sample from unit Ib. The inset graphs in (b) and (c) show example detail of the magnetic characteristics for uppermost sample.

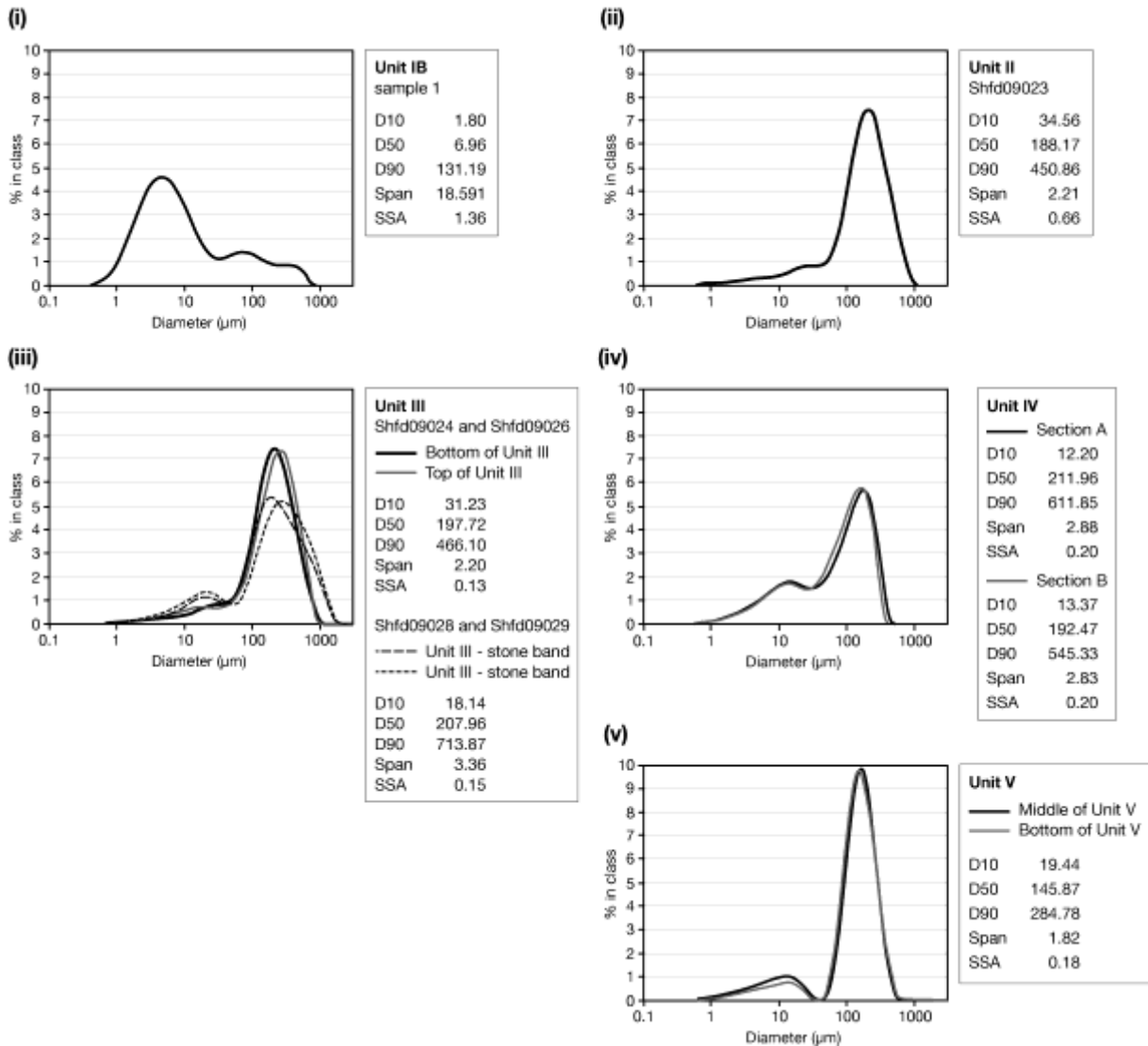


Fig. 7. (a) Particle size distributions outlining the grain size characteristics of the main sedimentary units at Soldier Mountain: (i) unit IB, (ii) the OSL samples taken from unit II, (iii) unit III, (iv) unit IV, and (v) unit V from sections A and B. Sample locations for the OSL samples used here can be found in Fig. 4. In each case, these samples represent particle size data for sediments that were not associated with stone horizons. Inset data refer to values for D10, D50 D90 (in mm), Span and SSA. (b) Particle size distributions for the samples taken from unit III that were subjected to an analysis of their environmental magnetism in order to establish the possibility that these were palaeosols; see Fig. 6 for sample locations. (i) sample location 5, (ii) sample location 4, (iii) sample location 3, and (iv) sample location 2. At each sample location c.10 sub-samples were collected at 5 cm intervals above, within and below stone horizons covering a total sample interval of 50 cm. In this case, sub-samples were averaged from 15 cm above, 20 cm within (middle), and 15 cm below the stone horizons to investigate particle size variability within the supposed 'palaeosols'.

specifically characterise the mineral magnetic signatures of sandy soils. While the former study demonstrated that frequency dependent magnetic susceptibility was enhanced in topsoil and in the finer soil fractions, it was undertaken in a cool temperate environment totally unlike that of the Mojave. The latter study, undertaken in Western Australia, failed to measure frequency dependent susceptibility as the initial measurements of low frequency susceptibility were too low to have confidence in the calculation of the frequency dependent signature. More recently, Lyons *et al.* (2012) reported results from a study of the mineral magnetic properties of dusts and sands in Niger in areas where annual rainfall minima are b100 mm in the north of the country. Lyons *et al.* (2012), and papers reviewed therein, confirm that a frequency-dependent susceptibility significantly greater than 2% would be strongly suggestive of the presence of magnetic grains at the superparamagnetic/sing domain boundary commonly associated with weathering and pedogenesis and their measurements of  $\chi_{fd}\%$  produced values significantly greater than 2%. They confirmed the presence of pedogenically

derived magnetic grains using a bivariate plot of  $\chi_{arm}/\chi_{fd}$  against  $\chi_{arm}/\chi_{lf}$  and compared this with a characteristic envelope curve of soils and palaeosols across Europe and Asia produced by Oldfield (2007) to confirm that most of their bulk and particle-size fractionated samples evidenced magnetic minerals produced by pedogenesis.

Field measurements of magnetic susceptibility ( $\kappa$ ) were made at 5-cm intervals on one profile (Fig. 4, profile A; Fig. 6) in order to sample across four potential palaeosols within unit III. Measurements were made using a Bartington Instruments MS2 susceptibility and MS2E surface scanning probe on freshly cleaned faces. A range of samples was also collected from selected units for particle size and further mineral magnetic analysis in the laboratory (see Fig. 4 profile A for sample locations).

In the laboratory samples were measured for their susceptibility and remanence properties, including low and high frequency magnetic susceptibilities. From these data frequency-dependent susceptibility, a number of remanence parameters (ARM,  $\chi_{arm}$  IRM0.88T, IRM loss after 24 h,

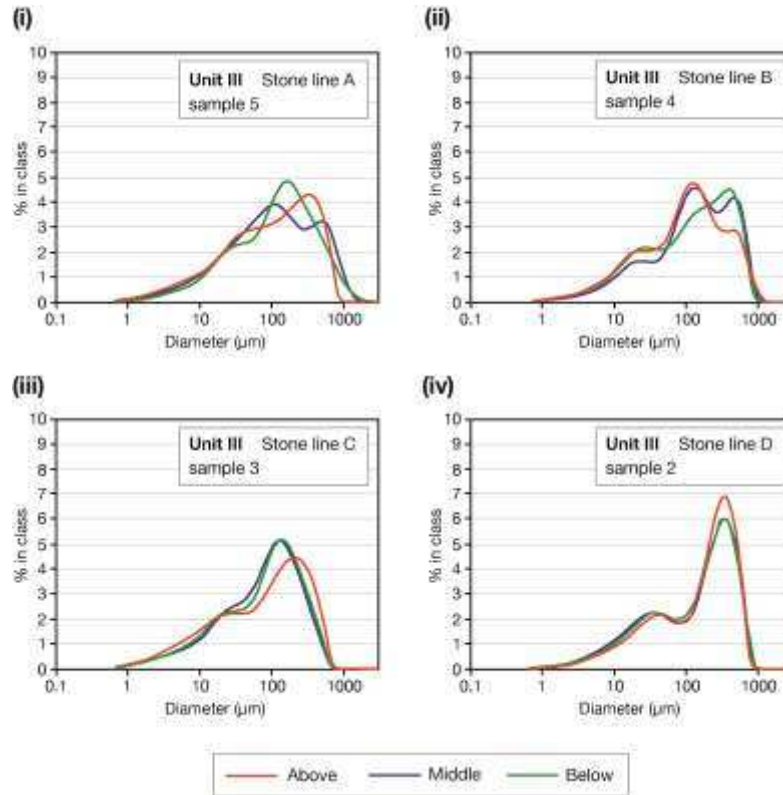


Fig. 7 (cont)

IRM-0.1T) and the S ratio and HIRM (mass-specific high field remanence; calculated as the difference between remanence at 0.88 and 0.1 T) were calculated. Details of the measurement and calculation methods are given by Walden *et al.* (1998), Foster *et al.* (2008) and Lyons *et al.* (2012).

Particle size analysis was undertaken in triplicate on all samples using a Malvern Mastersizer particle size analyser following destruction of organic matter, in order to establish whether mineral magnetic signatures were controlled by changes in the particle size distribution of the sediments. Several parameters describing particle size were extracted from the analysis (D10, D50 and D90; respectively, the diameter of the 10th, 50th and 90th percentiles of the distribution in microns), Span (a dimensionless sorting index;  $(D90-D10)/D50$ ) and the Specific Surface Area (calculated by assuming all particles in the particle size distribution are spherical ( $m^2 g^{-1}$ )) (Foster *et al.*, 1998).

## 6.2. Environmental magnetism results

Fig. 6a plots the down-profile  $\kappa$  signatures from profile A. This profile suggests that those layers which might be interpreted as 'palaeosols' have enhanced  $\kappa$  values by factors between 3 and 7 above underlying and overlying sedimentary units. Selected mineral magnetic signatures of the four 'palaeosols' analysed in detail (Fig. 6: samples 2 to 5) are presented in Fig. 6b/c and show significant enhancement in all susceptibility and remanence characteristics. All samples within these 'palaeosol' horizons were also found to have a much softer S-ratio ( $>0.60$ ), indicative of the presence of ferromagnetic minerals. However, unusually,  $\chi_{fd}\%$  values are barely detectable in these sections, with values reaching only a maximum of  $\sim 0.5\%$ , despite laboratory readings of volume susceptibility generally being well in excess of 30 and often exceeding 100. For comparative purposes, an analysis of the buried Lake Manix sediment measured a  $\chi_{fd}\%$  value of only 0.25% (see Fig. 6; sample 1). Enhancement of  $\chi_{fd}\%$  to values of

$\sim 8\%$  was used by Dearing *et al.* (2001), for example, to suggest the presence of palaeosols in the loess deposits of the Matmata plateau of central Tunisia, while Lyons *et al.* (2012) report significantly enhanced  $\chi_{fd}\%$  values in the dusts and sands of Niger to confirm the likely presence of pedogenic minerals and show that a large proportion of their samples plot within the envelope curve of palaeosols based on the bi-variate plot of  $\chi_{arm}/\chi_{fd}$  against  $\chi_{arm}/\chi_{lf}$ . Calculation of these ratios on samples taken from the Soldier Mountain sand ramp shows that none of them fall within this envelope curve. The presence of pedogenically-derived mineral magnetic grains is therefore not apparent in the supposed 'palaeosols' of the Soldier Mountain sand ramp.

The significant changes in both the  $\kappa$  profiles of Fig. 6a and the laboratory measurements of Fig. 6b/c could be interpreted as indicative of possible changes in the sediment sources contributing material to the Soldier Mountain sand ramp. However, many studies have shown that mineral magnetic signatures can be controlled by the particle size distribution of the sediments (Foster *et al.*, 1998; 2008) and this possible control on the mineral magnetic signatures is explored in the next section.

## 6.3. Particle size analysis

We present particle size data from the major units encountered at Soldier Mountain, as well as data associated with the stone horizons observed in unit III. Fig. 7a plots particle size distributions for unit IB (Fig. 7a (i)), and the OSL samples taken from unit II (Fig. 7a (ii)), unit III (Fig. 7a (iii)), unit IV (Fig. 7a (iv)) and unit V (Fig. 7a (v)) from sections A and B (see Fig. 4 for OSL and grain-size sample locations). Fig. 7b plots particle size distributions for the samples (sample 2-5) taken from unit III that were subjected to an analysis of their environmental magnetism in order to establish the possibility that they were from palaeosols (see Fig. 6 for sample locations).

From the summary particle size data it is evident that the underlying Lake Manix sediment from unit IA (Fig. 7a (i)) is significantly finer than the samples from any other unit sampled in the sequence, and has a dominant mode at or around 6–8  $\mu\text{m}$ . It has a small proportion of sediment coarser than 500  $\mu\text{m}$  which may indicate that this location was close to a littoral zone as it contains sediments too coarse to be transported to deep water. This material does not appear as a dominant component of the Soldier Mountain sand ramp, and is also magnetically distinctive from the overlying sand ramp sediments (see Fig. 6a). The fine sediments sampled within unit II (Fig. 7a (ii)) are relatively well sorted, have a D50 and dominant mode at around 190  $\mu\text{m}$ , and seem to be of predominantly aeolian origin. The sediments from the very top and bottom of unit III (Fig. 7a (iii)), are similar in nature and have a D50 and dominant mode at or around 200  $\mu\text{m}$ , and a subordinate mode and D10 at approximately 15–30  $\mu\text{m}$ . However, a marked increase in both D50 (>200  $\mu\text{m}$ ) and D90 (>700  $\mu\text{m}$ ), was observed near the stone horizon which suggests that there is an influx of coarse sand probably of non-aeolian origin associated with these horizons. Unit IV, which incorporates some lake-derived material, nevertheless has a D50 of 212  $\mu\text{m}$  (section A) and 192  $\mu\text{m}$  (section B); both of which are broadly comparable to the aeolian units directly below. The unit IV samples from both sections are not particularly well-sorted (Span>2.8), and while they do have an increase in the fine component (D10 12–13  $\mu\text{m}$ ), they show no evidence of the dominant fine mode apparent in unit 1B. Moving up to unit V (Fig. 7a (iv)), it was also observed that the particle size distribution becomes extremely well sorted (Span~1.8), with a dominant mode and D50 at approximately 145  $\mu\text{m}$ . This is consistent with interpretations of a uniform aeolian origin for this unit.

The particle size distributions of the samples from unit III collected at 5 cm increments across supposed 'palaeosol' horizons (Fig. 7b) fall into two distinct groups. The upper two 'palaeosols' (Fig. 6: samples 4 and 5; Fig. 7b (i) and (ii)) are extremely variable (with Span values of >4). These samples display tri-modal distributions with two modes at approximately 15  $\mu\text{m}$  and 120  $\mu\text{m}$ , which we have seen previously. In addition, these samples also have a mode at 400  $\mu\text{m}$ , which signifies an influx of sand that is unlikely to be of aeolian origin as noted earlier. Above and below the stone horizons at these locations (particularly in Fig. 7a (i) and (ii)) there is a transition in the particle size data, such that the presence of the 400  $\mu\text{m}$  mode diminishes as we go from samples between 15 cm below and above the stone horizon. The lower two 'palaeosols' (Fig. 6: samples 2 and 3; Fig. 7b (iii) and (iv)) are more consistently bimodal (Span values <3) with a dominant mode at ~300  $\mu\text{m}$  and ~130  $\mu\text{m}$ , respectively, and a common secondary mode at ~15–30  $\mu\text{m}$ . Here there is less variability in particle size as we move across the stone bands.

Overall, the high kappa, susceptibility and remanence properties within the 'palaeosols' in unit III of the sand ramp (see Fig. 6a) appear to be associated with sediments that have a coarse third mode in the particle size distribution. This association suggests a different sediment source from that of those sediments deposited elsewhere in unit III (and other units sampled). The fact that the sediments are coarser also supports the argument for an absence of palaeosols as the particle size distributions in 'palaeosols' would likely be finer than the potential 'parent' material found below from which these units would have been derived as a result of weathering and pedogenesis (e.g. Ellis and Mellor, 1995; Liu *et al.*, 2004). Importantly, throughout these data there was found to be no statistically significant correlation (p<0.05) between any of the magnetic signatures and the particle size characteristics of the deposited material at the sample sites.

#### 6.4. The significance of the sedimentology to the development of the Soldier Mountain sand ramp

Overall the sedimentological characteristics, encompassing environmental magnetic and particle size data, suggest that the sediments within the sand ramp may have been derived from a range of different sources. The sedimentological evidence and the discussion provided above certainly indicate that sand ramps accumulate sediment from local sources (proximal mountain fronts) as well as sources upwind of the site. While detailed source tracing work has yet to be undertaken on these sediments, mineral magnetic signatures are indicative of changes in sediment source over the timescale in which the ramp was formed.

Laboratory analysis of the magnetic and particle size signatures of aeolian sands within unit V provides further evidence to suggest a reasonably high level of internal uniformity and a common source. However we can see some divergence between this and aeolian sands in underlying units (e.g. II III and IV) which suggests that sources of aeolian sediments may have changed in the timescale of sand ramp formation. Based on the presence of ostracods, we can assume that reworking of Lake Manix sediments did occur in unit IV. However, based on grain size and mineral magnetic signatures we can see no further evidence for the incorporation of Lake Manix sediments in other units.

The possible presence of six 'palaeosols' in the Soldier Mountain sand ramp as suggested by Lancaster and Tchakerian (1996), Clarke and Rendell (1998) and Rendell and Sheffer (1996) is not confirmed by the mineral magnetic analysis of samples taken across 'palaeosol' boundaries. There appears to be some enhancement of several mineral magnetic signatures but these do not appear to be controlled by the presence of fine (0–0.03  $\mu\text{m}$ ) superparamagnetic grains that would be expected to contribute to a high frequency dependent signature (Lyons *et al.*, 2012). Rather, the trends in other parameters, such as the S-ratio, might indicate that these periods may have been associated with a change in sediment source rather than any period of protracted pedogenesis.

### 7. Stone movement within sand ramps

In the literature, the presence of discontinuous horizons of coarse rock fragments, at most a few fragments thick, has been attributed to four processes: (1) fluvial deposition, (2) debris-flow accumulations, (3) colluviation, and (4) stone horizon deposition. Lancaster and Tchakerian (1996) identify fluvial, debris-flow and stone horizon deposits within sand ramps in the Mojave Desert, of which the first is reported as being the most important, and occupying up to 42% of section thickness. For Soldier Mountain their figures are 8%, 3% and 5%, respectively. On Soldier Mountain, both fluvial and debris-flow deposits cut into pre-existing aeolian deposits, whereas the so-called stone horizon deposits clearly do not (Fig. 5c). Also the stone horizons at Soldier Mountain appear unsorted. Whether or not deflation contributes to the concentration of stones at the surface, the important issue is how they become redistributed in a layer of more-or-less uniform thickness over the surface of the sand ramp and, if similar layers of coarse particles within the aeolian deposits are also considered to be older desert pavements, how this redistribution might occur and how long it might take. To this end two approaches were undertaken. One uses regional data on downslope stone movement rates; the other employs monitoring contemporary stone movement on the Soldier Mountain sand ramp (Fig. 8).

#### 7.1. Stone movement rates

The particles both on and within the Soldier Mountain sand ramp are too coarse to be moved by shallow surface wash. Most likely, they move by a process of runoff creep (De Ploey and Moeyersons, 1975).



Fig. 8. An example of the emplacement (experimental site 1; see Fig. 3) of painted lines on the surface of the sand ramp directly south of Soldier Mountain. At this site the slope is 6°, with a slope orientation of 244°. Over a two year period the movement of each clast down-slope from the line was undertaken using the methods of Abrahams *et al.* (1984)

Their fabric is consistent with that investigated by Abrahams *et al.* (1990), which they attributed, in part at least, to runoff creep. On the assumption that these particles are moving in an analogous way to those investigated by Abrahams *et al.* (1990), rates of movement obtained by Abrahams *et al.* (1984) might be applied to obtain a first estimate of how long such surface layers might take to develop. These authors obtained a 16-year record of particle movement on debris slopes in the Apple Valley-Barstow area, approximately 60 km to the southwest of Soldier Mountain. The particles had a mean diameter of 55.5 mm, with a range of 8 to 300mm, and are thus comparable in size to those at Soldier Mountain which ranged from 1.5 to 320 mm. For these particles, Abrahams *et al.* (1984) derived two multiple regression equations to predict the movement *M* of the particles over the 16-year record of observation:

$$M = 34.67 X^{1.09} D^{-0.92} \text{ and } M = 9217^{1.5} D^{-1.01}$$

In which *D* is particle diameter (mm), *X* is distance to the divide (m) and *S* is the slope (tangent), with an *R*<sup>2</sup> of 0.44 and 0.32 respectively (and standard error of 0.46 and 0.54 log units). Applying Eq. (1) using a *D* of 55mm and *X* values between 10 and 50m (the general range observed by Abrahams *et al.*, 1984), we

can generate values of *M* between 0.7 mmyr<sup>-1</sup> (*X*=10) and 3.9mmyr<sup>-1</sup> (*X*=50). Applying Eq. (2) using an *S* equivalent to the maximum and minimum observed sand ramp slope angles (cf. Bertram, 2003; i.e. 4° and 25°), and a *D* of 55 mm allows us to predict that *M* will be in the region of 0.2 mm yr<sup>-1</sup> (4°) and 3.2 mm yr<sup>-1</sup> (25°). In either case, the maximum observable rate of movement for a typical clast would be unlikely to exceed 4 mm yr<sup>-1</sup>. Given that we have observed layers of angular clasts in our sections to be at least 50 m in horizontal distance from the mountain front from which they were derived, we could suggest that emplacement via runoff creep at this upper rate in a manner similar to that observed by Abrahams *et al.* (1984) could have taken as long as 12.5 ka. From Section 5 we can see that dates for the emplacement of the entire Soldier Mountain sand ramp would take considerably less time than this. Our dates suggest that the emplacement of unit III, with the highest concentration of layered coarse particles, took between 1.6 and 4.4 ka in total.

## 7.2. Contemporary stone movement monitoring

Given that the study by Abrahams *et al.* (1984) was undertaken on debris slopes and not on sand ramps, a real possibility exists that these rates cannot be applied to stone movement over sand. Consequently, as a test of the validity of applying the equations obtained by Abrahams *et al.* (1984) to the particles at Soldier Mountain, we obtained similar data over a 3-year period (2007–2010) for coarse particles (with diameter of 10–30 mm) at 8 sites on the surface of the undisturbed sand ramp directly south of the Soldier Mountain quarry. The sites stretched from the base of the sand ramp to the junction between the sand ramp and the mountain front. Slope angles varied from 6° (at the base) to 26° (at the junction). At each site a 3.5-m line of angular clasts perpendicular to the slope was painted (see Fig. 8). Movement of stones on each line was monitored annually using the approach of Abrahams *et al.* (1984) (see Table 4). The location of these sites is outlined in Fig. 3.

At each site we were able to compare our actual *M* values with those predicted using Eqs. (1) and (2). We can see from Fig. 9a that these data are not well matched when we invoke Eq. (1); partly perhaps as a function of the difficulty in determining distance to the divide on a sand ramp. By contrast, when we work with actual and predicted data based upon parameters which can be determined reliably in a field context (*S* and *D*) we can see from Fig. 9b that there is a reasonable match between the variables. However, although there is a good correlation between changes in observed and predicted rates, the former is over the order of three times greater than the latter suggesting that the process of runoff creep causes coarse particles to move over a sandy slope much faster than on a stony surface (and

Table 4. Details of data collected over three years at our eight experimental sites. For location of the study sites, see Fig. 4. *D* is b-axis diameter (mm) for material that moved, *X* is distance to the divide (m) and *S* is slope (tangent).

Site	<i>S</i> (degrees)	Orientation (degrees)	<i>X</i> (m) <sup>a</sup>	<i>D</i> (mm)	<i>M</i> (EQ1) predicted (mm/yr)	<i>M</i> (EQ2) predicted (mm/yr)	<i>M</i> -TOT obs Average total at site (mm)	<i>M</i> obs (mm/yr)
1	6.25	244	27	17.0	5.8	1.2	81.0	27.0
2	6	62	25	12.6	7.0	1.5	43.3	14.4
3	9	270	35	11.8	10.8	3.0	59.8	19.9
4	9.25	262	30	9.2	11.5	4.0	119.0	39.7
5	23	328	11	11.1	3.2	14.0	196.3	65.4
6	20	322	15	29.7	1.8	4.1	153.8	51.3
7	26	248	5	9.6	1.6	20.0	177.0	59.0
8	29	260	2	12.5	0.5	18.6	123.9	41.3

<sup>a</sup> estimated from aerial photographs.

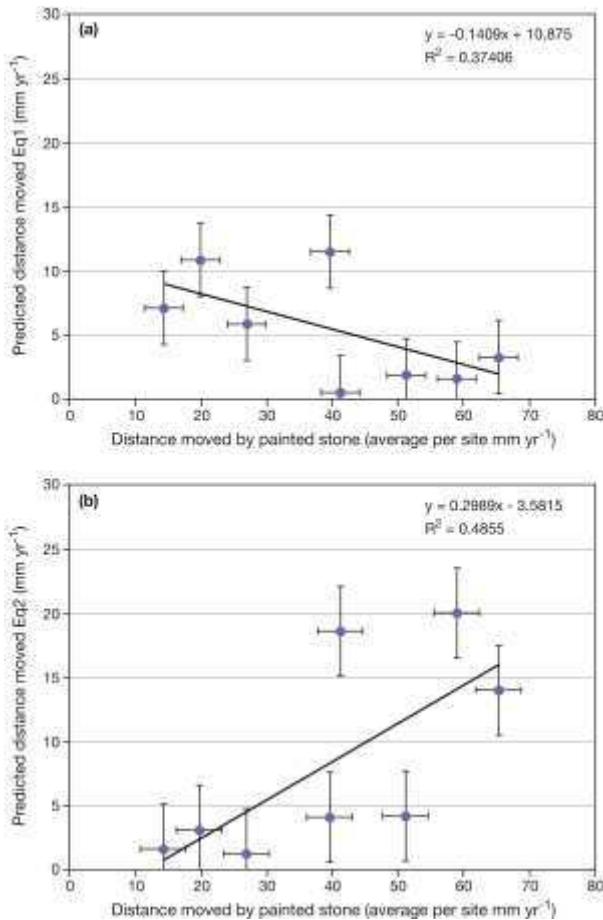


Fig. 9. A comparison between observed and predicted stone movement from collection of three years of data from our experiment using (a) Eq. (1), and (b) Eq. (2). Values used were average observed D and S (diameter and slope) at each site. Whiskers represent one standard error in the derivation of each equation as reported by [Abrahams et al. \(1984\)](#).

perhaps as much as 10 times faster for some sites — [Table 4](#); probably due to more ready undermining of the underlying sand. We therefore used the somewhat conservative regression outlined in [Fig. 9b](#) to recalibrate Eq. (2). Thus, using the previous D of 55 mm and slopes ranging between 4° and 25° we can attempt to revise upwards our estimates of M to between 0.6 and 11 mm yr<sup>-1</sup>. [Fig. 10](#) uses the same approach and equation to chart the time taken for clasts to move over the top surface of the Soldier Mountain ramp from the source (using slopes derived from cross section E in [Fig. 3](#)). These relatively conservative estimates suggest a time scale of up to 85 ka might be required. Even if we use the maximum transport rate and steepest slopes observed, travel of these clasts could have taken in the region of 4.5 ka to travel 50 m. If we are even more bold and use the suggestion (from [Fig. 9b](#)) that transport may have been more rapid than even this (perhaps up to ten times faster than on a stony surface; [Table 4](#)) we still struggle to emplace these layers within our sections in a time of less than 1.5 ka on a slope of 25° using a revised Eq. (2); a slope figure which is quite unlikely. Ultimately, even our most optimistic figures for stone transport over the surface of the sand ramp do not match well with either the overall chronological sequence observed at Soldier Mountain in which the new OSL chronology suggests all sand-ramp sedimentation took place within 85 ka and individual stone horizons

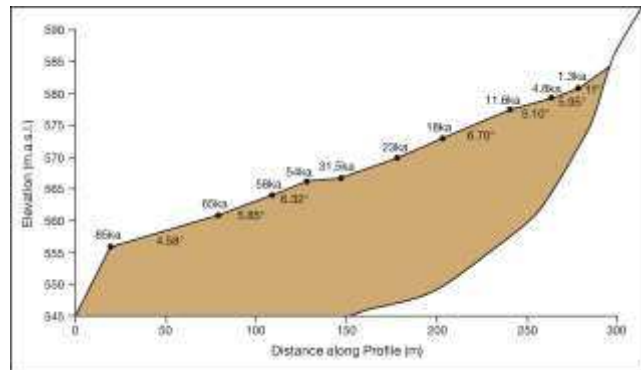


Fig. 10. A schematic cross-section of the Soldier Mountain sand ramp based on the surface topography found at transect E ([Fig. 3](#)). Shown are slope angles (degrees) and calculations of the possible time-scale (ka) required for the movement of clasts over the surface based on the equations derived from [Abrahams et al. \(1984\)](#), and stone movement rates on a neighbouring sand ramp.

## 8. Discussion

From the results presented here the evolution of the Soldier Mountain sand ramp can be discerned ([Fig. 11](#)). Prior to the formation of the sand ramp the area was covered by the high stand of Lake Manix forming unit 1b. When Lake Manix drained there is evidence at Soldier Mountain from ~15 ka of debris flows bringing weathered clastic material from the mountains forming unit II. This broadly fits with alluvial fan aggradation within the Mojave identified by [Miller et al. \(2010\)](#). Aeolian deposition at Soldier Mountain forming unit III occurred after 13.8 ka when Lake Manix and subsequently Lakes Coyote and Troy had dried up ([Reheis et al., 2007](#)). From then sediment became available for aeolian transportation from shoreline deposits, reworked deltaic and, once the river Mojave re-established itself, fluvial sediments ([Reynolds and Reynolds, 1994](#); [Reheis and Redwine, 2008](#)). Deposition of the sand ramp in this period fits well the phase 2 of Mojave sand ramp formation of [Kocurek and Lancaster \(1999\)](#). The final Aeolian phase (unit IV) saw free-form dunes moving across the sand ramp reflecting either increased aridity or that accommodation space at the mountain front had been filled by the sand ramp. Two further phases have occurred on the Soldier Mountain sand ramp since the final dune phase; the development of a stone-armoured surface across the top of unit IV and a phase of dissection when valleys were formed through the sand ramp. The latter may be related to the sustained flow identified in the medieval and Little Ice Age periods ([Miller et al., 2010](#)). That these valleys have not subsequently been infilled suggests that the sand ramp is now relict: either the whole system is moribund from an Aeolian perspective or is acting only as a transportation pathway with deposition elsewhere.

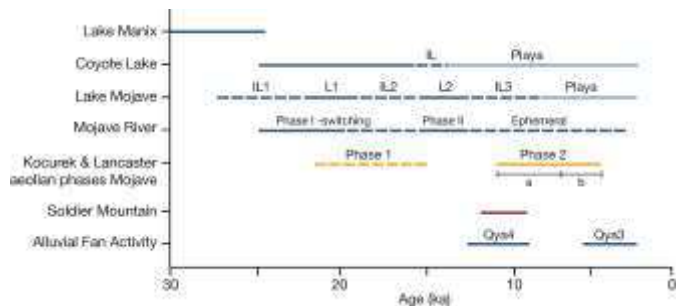


Fig. 11. Schematic summary of published regional lacustrine ([Reheis et al., 2007](#)), fluvial ([Reynolds and Reynolds, 1994](#)), alluvial ([Miller et al., 2010](#)) and aeolian ([Kocurek and Lancaster, 1999](#)) chronologies for the Manix/Mojave system. Ages have been calibrated into calendar years where appropriate.

The question remains as to the process responsible for the formation of the stone horizons. These can be separated into the stone horizon found completely covering the modern day surface of the entire sand ramp and those found intercalated within unit III.

For the modern stone surface, which may have had a considerable time to develop, the results presented above (Section 7) show that simple creep does not move stones sufficiently quickly for a clast to be moved from the mountain front across the sand ramp within the timeframe established.

Any process proposed for moving stones on the modern surface would have to include a mechanism for enhanced speed over and above the runoff creep found on rocky substrates (Abrahams *et al.*, 1984). For sand ramps, we propose an alternative process of fluvio aeolian creep. During wet events sufficient for localised overland flow, water would be concentrated around the margins of stone and could excavate finer sediment away from downslope side of stones causing them to be undermined and move downslope (i.e. runoff creep). Because of the greater proportion of fines compared to that found on debris slopes, it might be anticipated that this process would operate at an enhanced rate. Additionally, during intervening dry periods, wind (which here comes predominantly from the downslope side of the sand ramp and would be accelerated by the slope of the ramp itself) could deflate interstitial sand away from the downslope side of clasts to the upslope side again undermining clasts and also causing them to move downslope. While it might be thought that the ground-level wind velocity would be very low and insufficient to move sand between clasts, it is noted that the clasts forming the stone horizons are flat and tabular thus having a relatively low surface roughness but one in which sufficient near-surface turbulent flow to move sand-sized particles probably exists. That the three years of data thus far collected from the modern-day surface of Soldier Mountain show rates of movement an order of magnitude greater than creep on rock surfaces generally supports the concept of enhanced fluvio-aeolian creep. The mechanism would explain the occurrence of a stone horizon at the surface as with the observed creep rates there is just about sufficient time to move clasts across the entirety of the sand ramp within the Holocene period.

For the buried stone horizons within unit III, however, even this mechanism would not operate fast enough. Two potential mechanisms might operate during aeolian sedimentation; upwards net movement of pre-existing stones from the debris flow unit (unit II) or downslope localised redistribution of stones. With regard to the former, McFadden *et al.* (1987, 1998), in the context of Mojave Desert pavement development, suggested that volumetric changes induced by shrinking and swelling of clays and salts within sediments could allow cyclical vertical movement of surficial stone clastic layers, thereby allowing aeolian sediment to settle underneath the clasts. As a result, despite aeolian sedimentation, stones remain at the surface and are gradually raised up due to the accumulation of Aeolian sediment beneath them. However, four weaknesses exist in this explanation for the stone horizons within Soldier Mountain sand ramp. First, the new chronology associated with unit III indicates rapid aeolian sedimentation ( $>1$  m/ka), a rate at which it is hard to see how cyclical heaving of clasts could have kept pace. Secondly, as shown by the particle size data, relatively little clay exists to provide the shrinking and swelling within the sand matrix. Thirdly, even if this mechanism could lift stones up during aeolian sedimentation, if the source of all the clastic material was unit II this would account only for a single buried stone horizon (buried at the point when Aeolian accumulation exceeded stone uplift) or for the surface stones, not the multiple stone horizons observed within unit III. Finally, if this was the mechanism then the stone horizons would be found buried within a pure aeolian sediment matrix. As demonstrated by the particle size data (Fig. 7) there are clearly inputs of other sediment sources associated with the finematrix in which the stone horizons are found.

An alternative mechanism is that the stone horizons come from local downslope redistribution of clastic material. Observations show that actually most stone horizons are not laterally continuous beyond 10 m and that they do not always comprise a single stone thickness (they are up to a few stones thick). They could, therefore, represent deposits associated with periodic small streams moving stones and splaying them across the sand ramp. Such a mechanism (depending on climatic events being suitable to induce small streams) has the potential to deliver discontinuous stone horizons rapidly (depending on the exact stream pathway and competence to move across a highly porous surface) from the mountain front source on multiple occasions. This mechanism fits with the envisaged rapid accumulation of unit III of the sand ramp as it is not reliant on slow creep or creep-related mechanisms to move clasts from the mountain front and does not necessitate complete coverage of the sand ramp with clastic material. Particle size data for the matrix associated with the stone horizons also indicate a coarse non-aeolian mode of sufficient size that a fluvial original is more likely. Finally, features observed in unit III support this mechanism. From exposed sections in unit III perpendicular to the sand ramp, both stone-filled channels and stone horizons were observed. The former could represent flow which moved further downslope and the latter representing flow which was dissipating at this point of the slope and splaying. This interpretation assumes, among other things, that the original debris-flow phase (as represented by unit II) did not exhaust weathered material off mountain front or that weathering continues throughout so that stone horizons are not supply-limited.

Although the mechanisms suggested here solve some of the problems highlighted by the new data for processes previously put forward for sand ramp development, the proposed alternative mechanisms remain largely untested. At the moment modern-day stone monitoring covers only three relatively dry years so further measurements over a longer time period particularly before and after wetter years are required.

## 9. Conclusions

The above work shows that the sand ramps cannot easily be interpreted in terms of a simple model of fluctuating palaeoenvironmental phases from aeolian dominated to soil/fluvial dominated. A review of sand ramps and our research at Soldier Mountain indicates they accumulate quickly (perhaps in b5 ka), probably in a single phase before becoming relict. They appear strongly controlled by a 'window of opportunity' when plentiful sand is available and cease to develop when this sediment supply diminishes and/or the accommodation space is filled up. We interpret the stone horizons within sand ramps and the lack of evidence for soils as indicative of the interplay of high-magnitude, low-frequency weather events in which sand deposition was briefly interrupted, rather than phases of stability between phases of Aeolian accumulation. Contemporary data of stone movement both on rock and sandy sloping surfaces in the Mojave region indicate rates of movement of the order of 0.6 and 11 mm yr<sup>-1</sup>. This is not sufficiently fast to explain how stone horizons could have been formed on multiple occasions within b4 ka from the rock slopes behind the sand ramp to cover the sand ramp. Surface stone horizons may form by creep from mountain slope sources across sand ramps but require enhanced speed, proposed here to be due to fluvio-aeolian creep, in order to be established across the whole surface of a sand ramp. Our study suggests that existing models of alternating aeolian and colluvial deposition within sand ramps, their palaeoenvironmental significance and indeed how sand ramps are distinguished from other dune forms will require amendment.

## Acknowledgements

Fieldwork was partly funded by a grant to IL from the British Society for Geomorphology. The authors would like to thank Paul Coles for his assistance with drafting some of the figures and Rob Ashurst for his assistance with preparing material for luminescence dating. Janet Sherwin helped in the field. Dr Robert Fulton and his staff are thanked for providing excellent logistical support during fieldwork based at the Desert Studies Center at Zzyzx. Marith Reheis and Dave Miller (USGS Manolo) are also thanked for the many and varied discussions that ensued as this paper was being developed. Their sincere generosity and encouragement is noted. Finally we would like to thank the two anonymous reviewers and the journal editor, whose detailed comments and thoughts have helped improve the final manuscript.

## References

- Abrahams, A.D., Parsons, A.J., Cooke, R.U., Reeves, R.W., 1984. Stonemovement on hillslope in the Mojave Desert, California: a 16-year record. *Earth Surface Processes and Landforms* 9, 365–370.
- Abrahams, A.D., Soltyk, N., Parsons, A.J., Hirsch, P.J., 1990. Fabric analysis of a desert debris slope: Bell Mountain, California. *Journal of Geology* 98, 264–272.
- Avramov, V.I., Jordanova, D., Hoffmann, V., Roesler, W., 2006. The role of dust source area and pedogenesis in three loess-palaeosol sections from north Bulgaria: a mineral magnetic study. *Studia Geophysica et Geodaetica* 50, 259–282.
- Bertram, S., 2003. Late Quaternary sand ramps in south-western Namibia: nature, origin and palaeoclimatological significance. Unpublished doctoral thesis, Universität Würzburg. Available online at [http://www.opus-bayern.de/uni-wuerzburg/volltexte/2003/617/pdf/Dissertation\\_Silke\\_Bertram.pdf](http://www.opus-bayern.de/uni-wuerzburg/volltexte/2003/617/pdf/Dissertation_Silke_Bertram.pdf) accessed 04.05.11.
- Busche, D., 1998. Die zentrale Sahara - Oberflächenformen im Wandel. *Perthes Geographie im Bild*. Justus Perthes, Gotha. 284pp.
- Clarke, M.L., 1994. Infra-red stimulated luminescence ages from aeolian sand and alluvial fan deposits from the eastern Mojave Desert, California. *Quaternary Science Reviews* 13, 533–538.
- Clarke, M.L., Rendell, H.M., 1998. Climate change impacts on sand supply and the formation of desert sand dunes in the south-west USA. *Journal of Arid Environments* 39, 517–531.
- Clarke, M.L., Richardson, C.A., Rendell, H.M., 1996a. Luminescence dating of the Mojave Desert sands. *Quaternary Science Reviews* 14, 783–789.
- Clarke, M.L., Wintle, A.G., Lancaster, N., 1996b. Infra-red stimulated luminescence dating of sands from the Cronese Basins, Mojave Desert. *Geomorphology* 17, 199–206.
- Clemmensen, L.B., Fornós, J.J., Rodríguez-Perea, A., 1997. Morphology and architecture of a late Pleistocene cliff-front dune, Mallorca, Western Mediterranean. *Terra Nova* 9, 251–254.
- De Ploey, J., Moeyersons, J., 1975. Runoff creep of coarse debris: experimental data and some field observations. *Catena* 2, 275–288.
- Dearing, J.A., Dann, R.J.L., Hay, K., Lees, J.A., Loveland, P.J., Maher, B.A., O'Grady, K., 1996. Frequency-dependent susceptibility measurements of environmental materials. *Geophysics Journal International* 124, 228–240.
- Dearing, J.A., Livingstone, I.P., Bateman, M.D., White, K., 2001. Palaeoclimate records from OIS 8.0–5.4 recorded in loess-palaeosol sequences on the Matmata Plateau, Southern Tunisia, based on mineral magnetism and new luminescence dating. *Quaternary International* 76 (77), 43–56.
- Dokka, R.K., Travis, C.J., 1990. Late Cenozoic strike-slip faulting in the Mojave Desert, California. *Tectonics* 9, 311–340.
- Ellis, S., Mellor, A., 1995. *Soils and Environment*. Routledge, London, UK.
- Enzel, Y., Wells, S.G., Lancaster, N., 2003. Late Pleistocene lakes along the Mojave River, southeast California. In: Enzel, Y., Wells, S.G., Lancaster, N. (Eds.), *Paleoenvironments and paleohydrology of the Mojave and southern Great Basin Deserts: Geological Society of America Special Paper*, 368, pp. 61–77.
- Evans, M.E., Heller, F., 2001. Magnetism of loess-palaeosol sequences: recent developments. *Earth-Science Reviews* 54, 129–144.
- Evans, M.E., Heller, F., Bloemendal, J., Thouveny, N., 1997. Natural magnetic archives of past global change. *Surveys in Geophysics* 18, 183–196.
- Feng, Z.-D., Wang, H.B., Olson, C.G., 2004. Pedogenic factors affecting magnetic susceptibility of the last interglacial palaeosol S1 in the Chinese loess plateau. *Earth Surface Processes and Landforms* 29, 1389–1402.
- Foster, I.D.L., Lees, J.A., Owens, P.N., Walling, D.E., 1998. Mineral magnetic characterisation of sediment sources in the catchments of the Old Mill reservoir and Slapton Ley, South Devon, UK. *Earth Surface Processes and Landforms* 23, 685–703.
- Foster, I.D.L., Oldfield, F., Flower, R.J., Keatings, K., 2008. Mineral magnetic signatures of a long core from Lake Qarun, Middle Egypt. *Journal of Paleolimnology* 40, 835–849.
- Galbraith, R.F., Roberts, R.G., Laslett, G.M., Yoshida, H., Olley, J.M., 1999. Optical dating of single and multiple grains of quartz from Jinmium rock shelter, northern Australia: part I. experimental design and statistical models. *Archaeometry* 41, 339–364.
- Glazner, A.F., Walker, D.J., Bartley, J.M., Fletcher, J.M., 2002. Cenozoic evolution of the Mojave block of southern California. *Memoirs of the Geological Society of America* 195, 19–41.
- Jefferson, G.T., 2003. Stratigraphy and paleontology of the middle to late Pleistocene Manix Formation, and paleoenvironments of the central Mojave. In: Enzel, Y., Wells, S.G., Lancaster, N. (Eds.), *Paleoenvironments and paleohydrology of the Mojave and southern Great Basin Deserts: Geological Society of America Special Paper*, 368, pp. 43–60.
- Jordanova, D., Hus, J., Geeraerts, R., 2007. Palaeoclimatic implications of the magnetic record from loess/palaeosol sequence Viatovo (NE Bulgaria). *Geophysics Journal International* 171, 1036–1047.
- Kocurek, G., Lancaster, N., 1999. Aeolian sediment states: theory and Mojave Desert Kelso Dunefield example. *Sedimentology* 46, 505–516.
- Lamothe, M., Auclair, M., 1999. A solution to anomalous fading and age shortfalls in optical dating of feldspar minerals. *Earth and Planetary Science Letters* 171, 319–323.
- Lancaster, N., Tchakerian, V.P., 1996. Geomorphology and sediments of sand ramps in the Mojave Desert. *Geomorphology* 17, 151–165.
- Lancaster, N., Tchakerian, V.P., 2003. Late Quaternary eolian dynamics, Mojave Desert, California. In: Enzel, Y., Wells, S.G., Lancaster, N. (Eds.), *Geological Society of America Special Paper*, 368, pp. 231–249.
- Lian, O.B., Roberts, R.G., 2006. Dating the Quaternary: progress in luminescence dating of sediments. *Quaternary Science Reviews* 25, 2449–2468.
- Liu, Q., Jackson, M.J., Yu, Y., Chen, F., Deng, C., Zhu, R., 2004. Grain size distribution of pedogenic magnetic particles in Chinese loess/palaeosols. *Geophysical Research Letters* 31, L22603, <http://dx.doi.org/10.1029/2004GL021090>.
- Livingstone, I., Warren, A., 1996. *Aeolian Geomorphology: An Introduction*. Longman, Harlow.
- Lyons, R., Oldfield, F., Williams, E., 2012. The possible role of magnetic measurements in the discrimination of Sahara/Sahel dust sources. *Earth Surface Processes and Landforms*, <http://dx.doi.org/10.1002/esp.2268>.
- Maher, B.A., 1986. Characterisation of soils by mineral magnetic measurements. *Physics of the Earth and Planetary Interiors* 42, 76–92.
- Maher, B., Thompson, R., Zhou, L.P., 1994. Spatial and temporal reconstructions of changes in the Asian palaeomonsoon: a new mineral magnetic approach. *Earth and Planetary Science Letters* 125, 461–471.
- Maher, B.A., MengYu, H., Roberts, H.M., Wintle, A.G., 2003. Holocene loess accumulation and soil development at the western edge of the Chinese Loess Plateau: implications for magnetic proxies of palaeorainfall. *Quaternary Science Reviews* 22, 445–451.
- McFadden, L.D., Wells, S.G., Jercinovich, M.J., 1987. Influences of eolian and pedogenic processes on the origin and evolution of desert pavements. *Geology* 15, 504–508.
- McFadden, L.D., McDonold, E.V., Wells, S.G., Anderson, K., Quade, J., Forman, S.L., 1998. The vesicular layer and carbonate collars of desert soils and pavements: formation age and relation to climate change. *Geomorphology* 24, 101–145.
- Meek, N., 1989. Geomorphic and hydrologic implications of the rapid incision of Afton Canyon, Mojave Desert, California. *Geology* 17, 7–10.
- Meek, N., 1999. New discoveries about the Late Wisconsinan history of the Mojave River system. In: Reynolds, R.E., Reynolds, J. (Eds.), *Tracks along the Mojave: A Field Guide from Cajon Pass to the Calico Mountains and Coyote Lake: San Bernardino Museum Quarterly*, v. 46, pp. 113–117.
- Meek, N., 2004. Mojave River history from an upstream perspective. In: Reynolds, R.E. (Ed.), *Breaking Up—The 2004 Desert Symposium Field Trip and Abstracts: Fullerton, California, California State University, Desert Studies Consortium*, pp. 41–49.
- Miller, D.M., Dudash, S.L., 2009. Chronology of pluvial Lake Coyote, California, and implications for Mojave River paleohydrology. In: Jessey, D.R., Reynolds, R.E. (Eds.), *Landscape Evolution at an Active Plate Margin, Desert Studies Consortium*. California State University, and LSA Associates, Inc., Riverside, p. 205.
- Miller, D.M., Schmidt, K.M., Mahan, S.A., McGeehin, J.P., Owen, L.A., Barron, J.A., Lehmkuhl, F., Lohrer, R., 2010. Holocene landscape response to seasonality of storms in the Mojave Desert. *Quaternary International* 215, 45–61.
- Murray, A., Wintle, A., 2003. The single aliquot regenerative dose protocol: potential for improvements in reliability. *Radiation Measurements* v. 37, 377–381.
- Nash, D.J., 2011. *Desert Crusts and Rock Coatings*. In: Thomas, D.S.G. (Ed.), 3rd edition. Wiley-Blackwell, Chichester, UK, pp. 131–180.
- Newsome, D., Walden, J., 2000. Mineral magnetic evidence for heterogeneous sandplain regolith in Western Australia. *Journal of Arid Environments* 45, 139–150.

- Oldfield, F., 2007. Sources of fine-grained magnetic minerals in sediments: a problem revisited. *The Holocene* 17, 1265–1271.
- Prescott, J.R., Hutton, J.T., 1994. Cosmic ray contributions to dose rates for luminescence and ESR dating: large depths and long-term variations. *Radiation Measurements* 23, 497–500.
- Reheis, M.C., Redwine, J.L., 2008. Lake Manix shorelines and Afton Canyon terraces: implications for incision of Afton Canyon. In: Reheis, M.C., Hershler, R., Miller, D. (Eds.), *Late Cenozoic drainage history of the southwestern Great Basin and Lower Colorado River Region: geologic and biotic perspectives*. Geological Society of America Special Paper, 439, pp. 227–259. [http://dx.doi.org/10.1130/2008.2439\(10\)](http://dx.doi.org/10.1130/2008.2439(10)).
- Reheis, M.C., Miller, D.M., Redwine, J.L., 2007. Quaternary stratigraphy, drainage-basin development, and geomorphology of the Lake Manix Basin, Mojave Desert — guidebook for fall field trip, friends of the Pleistocene, Pacific Cell. U.S. Geological Survey (Open-File Report 2007-1281, 31pp.).
- Rendell, H.M., Sheffer, N.L., 1996. Luminescence dating of sand ramps in the Eastern Mojave Desert. *Geomorphology* 17, 187–197, [http://dx.doi.org/10.1016/0169-555X\(95\)00102-B](http://dx.doi.org/10.1016/0169-555X(95)00102-B).
- Rendell, H.M., Lancaster, N., Tchakerian, V., 1994. Luminescence dating of Late Quaternary aeolian deposits at Dale Lake and Cronese Mountains, Mojave Desert, California. *Quaternary Geochronology* 13, 417–422.
- Reynolds, R.E., Reynolds, R.L., 1994. The isolation of Harper Lake Basin. Special Publication, 94–1. San Bernardino County Museum Association, pp. 34–37.
- Sandgren, P., Thompson, R., 1990. Mineral magnetic characteristics of podzolic soils developed on sand dunes in the Lake Goszias catchment, central Poland. *Physics of Earth and Planetary Interiors* 60, 297–313.
- Selby, M.J., 1993. *Hillslope Materials and Processes*, second edition. University Press, Oxford.
- Singer, M.J., Verosub, K.L., Fine, P., TenPas, J., 1996. A conceptual model for the enhancement of magnetic susceptibility in soils. *Quaternary International* 34–36, 243–248.
- Tchakerian, V.P., 1991. Late Quaternary eolian geomorphology of the Dale Lake sand sheet, southern Mojave Desert, California. *Physical Geography* 12, 347–437.
- Tchakerian, V.P., Lancaster, N., 2002. Late Quaternary arid/humid cycles in the Mojave Desert and western Great Basin of North America. *Quaternary Science Reviews* 21, 799–810.
- Telfer, M.W., Thomas, Z.A., Breman, B., 2012. Sand ramps in the Golden Gate Highlands National Park, South Africa: evidence of periglacial aeolian activity during the Last Glacial. *Palaeogeography, Palaeoclimatology, Palaeoecology* 313–4, 59–69.
- Thomas, D.S.G., Bateman, M.D., Mehrshahi, D., OHara, S.L., 1997. Development and environmental significance of an eolian sand ramp of last-glacial age, central Iran. *Quaternary Research* 48, 155–161.
- Turner, B.R., Makhlof, I., 2002. Recent colluvial sedimentation in Jordan: fans evolving into sand ramps. *Sedimentology* 49, 1283–1298. *Environmental magnetism — a practical guide*. In: Walden, J., Oldfield, F., Smith, J. (Eds.), *Quaternary Research Association Technical Guide No 6*. London QRA.
- Wells, S.G., Brown, W.J., Enzel, Y., Anderson, R.Y., McFadden, L.D., 2003. Late Quaternary geology and paleohydrology of pluvial Lake Mojave, southern California. In: Enzel, Y., Wells, S.G., Lancaster, N. (Eds.), *Paleoenvironments and paleohydrology of the Mojave and southern Great Basin Deserts*: Geological Society of America Special Paper, 368, pp. 79–114.
- Zimbelman, J.R., Williams, S.H., Tchakerian, V.P., 1995. Sand transport paths in the Mojave Desert, southwestern United States. In: Tchakerian, V.P. (Ed.), *Desert Aeolian Processes*. Chapman and Hall.